Multi-Level Power-Imbalance Allocation Control for Secondary Frequency Control of Power Systems

Xi, Kaihua; Lin, Hai Xiang; Shen, Chen; van Schuppen, Jan

DOI
10.1109/TAC.2019.2934014

Publication date
2020

Document Version
Accepted author manuscript

Published in
IEEE Transactions on Automatic Control

Citation (APA)
Xi, K., Lin, H. X., Shen, C., & van Schuppen, J. (2020). Multi-Level Power-Imbalance Allocation Control for Secondary Frequency Control of Power Systems. *IEEE Transactions on Automatic Control*, *65*(7), 2913-2928. Article 8792146. https://doi.org/10.1109/TAC.2019.2934014

This article has been accepted for publication in a future issue of this journal, but has not been fully edited. Content may change prior to final publication. Citation information: DOI 10.1109/TAC.2019.2934014, IEEE Transactions on Automatic Control

Multi-Level Power-Imbalance Allocation Control for Secondary Frequency Control of Power Systems

Kaihua Xi, *Member, IEEE,* Hai Xiang Lin, Chen Shen, *Senior member, IEEE,* Jan H. van Schuppen, *Life member, IEEE*

***Abstract*—A consensus-control-based multi-level control law named *Multi-Level Power-Imbalance Allocation Control* (MLPIAC) is presented for a large-scale power system partitioned into two or more groups. Centralized control is implemented in each group while distributed control is implemented at the coordination level of the groups. Besides restoring nominal frequency with a minimal control cost, MLPIAC can improve the transient performance of the system through an accelerated convergence of the control inputs without oscillations. At the coordination level of the control groups, because the number of the groups is smaller than that of nodes, MLPIAC is more effective to obtain the minimized control cost than the purely distributed control law. At the level of the control in each group, because the number of nodes is much smaller than the total number of nodes in the whole network, the overheads in the communications and the computations are reduced compared to the pure centralized control. The asymptotic stability of MLPIAC is proven using the Lyapunov method and the performance is evaluated through simulations.**

***Index Terms*—Economic Power Dispatch, Centralized Control, Distributed Power-Imbalance Allocation Control, Multi-Level control, Transient performance**

I. Introduction

Power systems need to be controlled to provide alternating current with nominal frequency, 60 Hz in the USA, and 50 Hz in the main parts of Europe and in Asia. The power demand fluctuates continuously due to switching on or off loads. Consequently, the frequency of the power systems also fluctuates continuously. Hence the power systems must be controlled to maintain the frequency as close as possible to the agreed reference value.

There are three forms of control: primary, secondary, and tertiary frequency control which are distinguished based on fast to slow time-scales [15]. Primary frequency control synchronizes the frequencies of synchronous machines and balances the power supply and demand of the power system at a small time-scale. However, the synchronized frequency may deviate from its nominal value. Secondary frequency control restores the nominal frequency at a medium time-scale. With a prediction of power demand, tertiary control calculates the operating point stabilized by primary and secondary control at a large time-scale, which concerns the security and economy of the power system [36].

The focus of this paper is on the secondary frequency control, which is implemented by *Automatic Generation Control* (AGC). AGC is driven by *Area Control Error* (ACE) which is calculated from the local frequency deviation within an area and power flow deviations of the tie-line between its neighbor areas [15], [22]. By controlling the power generation, AGC steers the ACE to zero thus restores the nominal frequency. We consider power systems with lossless transmission lines, which comprise traditional synchronous machines, frequency dependent devices, e.g., power inverters of renewable energy or frequency dependent loads, and passive loads. The control objectives can be described as: restore the frequency to its nominal value and minimize the control cost of the power system. Due to the availability of communication networks, the initial approach to control synthesis of secondary frequency control is to apply centralized control [7], [32], [42], where a central controller collects state information via a communication network and computes the control inputs for the local actuators. The minimal control cost is achieved by solving an economic power dispatch problem. In practice today's power systems are becoming so large that they cannot be effectively controlled by a centralized controller. The communication overhead and the control computations carried out at the central controller take so much time that the control objectives cannot be satisfactorily achieved. In addition, the centralized control does not effectively meet the requirement of the system integrated with a large amount of distributed power sources.

Therefore, a form of distributed control is proposed for control of power systems, which are either based on passivity method [20], [38], [17], [30], [28], [26], [27] or primal-dual method [43], [16], [44], [35]. In distributed control of a power system, a number of controllers aim to achieve the control objectives of the entire network via coordination and cooperation. The state information and control inputs are collected and computed by the local controller at each node. In order to minimize the control cost, the controllers need to exchange control information with their neighboring controllers via the communication network. However, this suffers from a slow convergence to the optimal steady state because of the large scale of the power system.

In addition, these centralized and distributed control usually focus on the steady state only. The transient performance

In this work, Kaihua Xi is supported by the Foundation for Innovative Research Groups of National Natural Science Foundation (61821004) and the Fundamental Research Funds of Shandong University (2018HW028).

Kaihua Xi is with the school of mathematics, Shandong University, Jinan, 250100, China (e-mail: kxi@sdu.edu.cn).

Hai Xiang Lin and Jan H. van Schuppen are with Delft Institute of Applied Mathematics, Delft University of Technology, 2628CD, Delft, The Netherlands (e-mail: {H.X.Lin, J.H.vanSchuppen}@tudelft.nl).

Chen Shen is with the State Key Laboratory of Power Systems, Department of Electrical Engineering, Tsinghua University, Beijing, 10084, China (email: shenchen@mail.tsinghua.edu.cn).

Corresponding author: Kaihua Xi.

This article has been accepted for publication in a future issue of this journal, but has not been fully edited. Content may change prior to final publication. Citation information: DOI 10.1109/TAC.2019.2934014, IEEE Transactions on Automatic Control

is seldom considered when designing the control algorithms. During the transient phase, *extra frequency oscillations* or *slow convergence* to the steady state may be introduced due to the control algorithms [12], [9], [4], which should be avoided for a high quality power supply by the power systems with various disturbances. The traditional way to improve the transient performance is to tune the control gain coefficients through eigenvalue or $\mathcal{H}_2/\mathcal{H}_\infty$ norm analysis [37], [5], [24]. However, besides the complicated computations, these methods focus on the linearized system only and the improvement of the transient performance is still limited because it also depends on the structure of the control algorithms. In order to improve the transient performance, sliding mode based control laws, e.g., [34], [18], and fuzzy control based control laws, e.g., [10], are proposed, which are able to shorten the transient phase without the extra oscillations. However, those control laws use either centralized control or decentralized control without considering economic power dispatch. In order to improve the transient performance and optimize the control cost, *Power-imbalance Allocation Control* (PIAC) is proposed in [42]. By tuning a control gain coefficient, the convergence of the system can be accelerated without introducing extra frequency oscillations. However, it is a centralized control law, which suffers from the disadvantages of centralized control.

The power system usually has a multi-level structure [15]. For example, the systems at the level of communities are subsystems of the systems at the level of provinces, which are further subsystems at a higher level of the states. Control methods for this kind of multi-level power systems are seldom considered.

In this paper, we aim to synthesize a multi-level control law for secondary frequency control of large-scale power systems with a multi-level structure, which is able to balance the advantages and disadvantages of the centralized and distributed control, and eliminates the extra frequency oscillations and the slow convergence problem. The control objective is the same as that of PIAC and can be described as: restore the frequency to its nominal value, prevent the extra frequency oscillations caused by the controllers, and minimize the economic cost in the operation of the power systems.

The contributions of this paper include:

(i) a multi-level control law, *Multi-Level Power-Imbalance Allocation Control* (MLPIAC), is proposed, which is not only able to balance the advantages and disadvantages of centralized and distributed control, but also suitable for power systems with a multi-level structure.
(ii) the control cost is minimized and both the transient performance of the frequency and of the control cost can be improved by tuning three gain parameters in MLPIAC.
(iii) the Lyapunov stability analysis and a case study are provided to evaluate the asymptotic stability and performance of MLPIAC.

Not discussed because of limitations of space are robustness of the closed-loop system, the interaction between frequency control and voltage control, the noise and time delays in the communications and frequency measurement.

This paper is organized as follows. We describe the dynamic model of the power network and formulate the problem in Section II. We synthesize MLPIAC with transient performance analysis in Section III. The asymptotic stability is analysed in Section IV and the performance of MLPIAC is evaluated in the case study in Section V. Concluding remarks are given in Section VI.

II. Dynamic model and secondary control

A power network is described by a graph $\mathcal{G} = (\mathcal{V}, \mathcal{E})$ with nodes $\mathcal{V}$ and edges $\mathcal{E} \subseteq \mathcal{V} \times \mathcal{V}$ where a node represents a bus and edge (i, j) represents the direct transmission line connection between node i and j. The buses are connected to synchronous machines, frequency dependent power sources (e.g., power inverters of renewable energy) or loads, or passive loads. The resistance of the transmission lines are neglected and the susceptance is denoted by $\hat{B}_{ij}$. Denote the set of the buses of the synchronous machines, frequency dependent power sources, passive loads by $\mathcal{V}_M, \mathcal{V}_F, \mathcal{V}_P$ respectively, thus $\mathcal{V} = \mathcal{V}_M \cup \mathcal{V}_F \cup \mathcal{V}_P$.

The dynamic model of the power system is described by the following *Differential Algebraic Equations* (DAEs), e.g.,[7],

$$\dot{\theta}_i = \omega_i, \ i \in \mathcal{V}_M \cup \mathcal{V}_F, \tag{1a}$$

$$M_i\dot{\omega}_i = P_i - D_i\omega_i - \sum_{j\in\mathcal{V}} B_{ij}\sin(\theta_i - \theta_j) + u_i, i \in \mathcal{V}_M, \tag{1b}$$

$$0 = P_i - D_i\omega_i - \sum_{j\in\mathcal{V}} B_{ij}\sin(\theta_i - \theta_j) + u_i, i \in \mathcal{V}_F, \tag{1c}$$

$$0 = P_i - \sum_{j\in\mathcal{V}} B_{ij}\sin(\theta_i - \theta_j), i \in \mathcal{V}_P, \tag{1d}$$

where θ_i is the phase angle at node i, ω_i is the frequency deviation from the nominal frequency, i.e., $f^* = 50$ or 60 Hz, $M_i > 0$ is the moment of inertia of the synchronous machine, D_i is the droop control coefficient, P_i is the power generation (or demand), $B_{ij} = \hat{B}_{ij}V_iV_j$ is the effective susceptance matrix, V_i is the voltage, u_i is the secondary control input. We assume that the nodes participating in secondary frequency control are equipped with primary controllers. Denote the set of the nodes equipped with the secondary controllers by $\mathcal{V}_K$, thus $\mathcal{V}_K = \mathcal{V}_M \cup \mathcal{V}_F$. Since the control of the voltage and the frequency can be decoupled, we do not model the dynamics of the voltages and assume the voltage of each bus is a constant which can be derived from power flow calculation [15]. In practice, the voltage can be well controlled by Automatic Voltage Regulator (AVR). This model and the ones with linearized sine function are widely studied, e.g.,[7], [8], [30], [23], [26], [44], [16], in which the frequency dependent nodes are usually used to model the renewable power inverters.

The system (1) synchronizes at an equilibrium state, called *synchronous state* defined as follows [6].

Definition 2.1: A steady state of the power system (1) with

This article has been accepted for publication in a future issue of this journal, but has not been fully edited. Content may change prior to final publication. Citation information: DOI 10.1109/TAC.2019.2934014, IEEE Transactions on Automatic Control

constant power loads (generation) yields,

$$\omega_i = \omega_{syn},\ i \in \mathcal{V}_M \cup \mathcal{V}_F \tag{2a}$$
$$\dot{\omega}_i = 0,\ i \in \mathcal{V}_M \cup \mathcal{V}_F, \tag{2b}$$
$$\theta_i = \omega_{syn} t + \theta_i^*,\ i \in \mathcal{V}, \tag{2c}$$
$$\dot{\theta}_i = \omega_{syn}, \tag{2d}$$

where θ_i^* is the phase angle of node i at the steady state, $\omega_{syn} \in \mathbb{R}$ is the synchronized frequency deviation.

Note that the angle differences $\{\theta_{ij}^* = \theta_i^* - \theta_j^*,\ i, j \in \mathcal{E}\}$ determine the power flows in the transmission lines. Substituting (2) into the system (1), we derive the explicit formula of the synchronized frequency deviation as

$$\omega_{syn} = \frac{\sum_{i\in\mathcal{V}} P_i + \sum_{i\in\mathcal{V}_K} u_i}{\sum_{i\in\mathcal{V}_M\cup\mathcal{V}_F} D_i}. \tag{3}$$

The *power imbalance* is defined as $P_s = \sum_{i\in\mathcal{V}} P_i$. In order to avoid damages to electrical devices in the system, the frequency deviation should be zero, i.e., $\omega_{syn} = 0$, for which the necessary condition is

$$P_s + \sum_{i\in\mathcal{V}_K} u_i = 0,$$

which can be satisfied by the set $\{u_i,\ i \in \mathcal{V}_K\}$ of control inputs determined by a control law. We aim to synthesize an effective secondary frequency control law to control ω_{syn} to zero with a minimal control cost, that requires solving the following economic power dispatch problem,

$$\min_{\{u_i\in\mathbb{R}, i\in\mathcal{V}_K\}} \sum_{i\in\mathcal{V}_K} \frac{1}{2}\alpha_i u_i^2, \tag{4}$$
$$s.t.\ \ P_s + \sum_{i\in\mathcal{V}_K} u_i = 0,$$

where $\alpha_i \in \mathbb{R}$ is a positive constant and denotes the control price of node i [36].

Regarding to the existence of a feasible solution of the optimization problem (4), we make the following assumption.

Assumption 2.2: Consider the system (1) with the economic power dispatch problem (4), assume

(i) the power supply and demand are constant in a small time interval, thus P_s is a constant.

(ii) the power imbalance can be compensated by the control inputs such that

$$-P_s \in \Big[\sum_{i\in\mathcal{V}_K} \underline{u}_i, \sum_{i\in\mathcal{V}_K} \overline{u}_i\Big]$$

In practice, the power imbalance is not constant but continuously fluctuating due to the uncertain behaviour of consumers [41]. However, the time-scale of the secondary frequency control is small, the power imbalance be viewed as a constant. Furthermore, for the synthesis of the control laws, it is common to assume the power demand as a constant [13] as in Assumption 2.2 (i). On the power supply side, tertiary control calculates the operating point of P_i in a small time interval, which is stabilized by secondary frequency control. In general, the electricity demand can be satisfied. So Assumption 2.2 (ii) is realistic.

A necessary condition for the optimal solution of (4) is

$$\alpha_i u_i = \alpha_j u_j = \lambda,\ i, j \in \mathcal{V}_K \tag{5}$$

where $\alpha_i u_i$ is the *marginal cost* of node i and λ is the *nodal price*. With this condition, if the power-imbalance P_s is known, the optimization problem (4) can be solved analytically. However, P_s is unknown in practice since the loads cannot be predicted precisely in a short time interval.

After a disturbance, the state of the power system experiences two phases: a transient phase and a steady phase. In a centralized control law, e.g., [7], [42], the nodal price estimated by the central controller is broadcast to the local controllers which calculate the control inputs according to (5). So the marginal costs are all identical during the transient phase. However, the central controller suffers from the communication overhead with the local controllers and intensive computations. In distributed secondary frequency control, the principle of consensus control is used to let the marginal costs of all nodes achieve a consensus at the steady state [1]. Because the nodes communicate with their neighbours and compute the control input locally, the communications and computations are greatly reduced. However, this sacrifices the performance of the marginal costs, i.e., they are not identical during the transient phase leading to increase in the control cost. Furthermore, the consensus speed decreases as the scale of the network increases, which further increases the control cost.

The existing control laws usually consider the steady state only. The extra frequency oscillations or slow convergence to the steady state may be introduced by the controllers due to the control algorithms [12], [9], [4], which deteriorate the transient performance of the system. The dynamics of actuators of the power system may be included into the model (1) [31]. The extra frequency oscillation may be reduced by having a slow actuator dynamics but then the frequency deviation will be large from the nominal value. If the actuator dynamics is very fast then there is little difference from the case without actuator dynamics. Therefore, the actuator dynamics does not eliminate the extra oscillation and large frequency deviation which are mainly due to the control algorithms.

In this paper, besides the optimization problem (4) for secondary frequency control, we also focus on the transient performance of the power system. We consider the following problem.

Problem 2.3: Consider a large-scale power system described by (1). Design a secondary frequency control law so as to improve the transient performance with a minimal control cost, i.e., eliminate the extra frequency oscillation caused by the oscillations of the control inputs and accelerate the convergence of the optimization of control cost.

PIAC proposed in [42] is able to eliminate the extra frequency oscillation, which however is a centralized control and cannot be applied to large-scale power systems. In the next Section, we propose a multi-level control law which is a trade-off between centralized and distributed control and thus solve Problem 2.3. In order to solve the optimization problem (4), a communication network connecting the controllers is required, for which we make the following assumption.

This article has been accepted for publication in a future issue of this journal, but has not been fully edited. Content may change prior to final publication. Citation information: DOI 10.1109/TAC.2019.2934014, IEEE Transactions on Automatic Control

Assumption 2.4: Consider the power system (1), assume all the nodes in the set $\mathcal{V}_K$ are connected by a communication network.

This assumption can be satisfied if there is at least a spanning tree communication network connecting the nodes. The communication network might be unreliable with noise and time-delays, which are not considered in this paper.

III. Multilevel control approach

First, with respect to the transient performance of frequency, we decompose the frequency deviation into two types, i.e., global frequency deviation and relative frequency deviation between the nodes. The transient performance of relative frequency deviation can be improved by primary control [21]. So we focus on improving the transient performance of the global frequency deviation. It can be observed from (3) that the global frequency deviation at the steady state is determined by the power-imbalance and the total damping of the system. Because of the heterogeneity of M_i and D_i, it is hard to qualify the performance of the global frequency deviation during the transient phase. To treat the transient performance we define an abstract frequency deviation to measure the global frequency deviation as follows.

Definition 3.1: For the power system (1), define an abstract frequency deviation ω_s [42] which is assumed to be a solution of the following equation,

$$M_s\dot{\omega}_s = P_s - D_s\omega_s + u_s \tag{6}$$

where $M_s = \sum_{i\in\mathcal{V}_M} M_i$ denotes effective inertia, $D_s = \sum_{i\in\mathcal{V}} D_i$ denotes effective droop control coefficient, and $u_s = \sum_{i\in\mathcal{V}_K} u_i$ denotes the total control input of the system.

$\omega_s(t)$ is different from $\omega_i(t)$ and $\omega_{syn}(t)$. It can be easily obtained that $\omega_s^* = \omega_{syn} = \omega_i$ at the steady state. The dynamics of ω_s involves the total inertias, droop control coefficients and power-imbalance, so it is reasonable to use ω_s to study the transient performance of the global frequency deviation.

Second, regarding to the distributed control, we partition the network denoted by A into m groups such that

$$A = A_1 \cup \cdots \cup A_r \cup \cdots \cup A_m,\ Z_m = \{1, 2, \cdots, m\}, \tag{7a}$$

$$A_r \cap A_q = \emptyset,\ r \neq q,\ r,\ q \in Z_m. \tag{7b}$$

There is a group controller in each group. Denote the set of the nodes in group A_r by $\mathcal{V}_{A_r}$, the nodes of the synchronous machines by $\mathcal{V}_{M_r}$, the nodes of the frequency dependent power sources by $\mathcal{V}_{F_r}$, the nodes with secondary controller by $\mathcal{V}_{K_r}$, the marginal cost of group A_r by λ_r, and the set of the neighboring groups of A_r connected by communication line as Z_{m_r}.

We remark that in traditional multi-area control the power flow of the tie-lines between areas should be restored to its nominal value after a disturbance [15, chapter 11], where each area cares about its own power-imbalance only. Thus the control cost of the system cannot be minimized at the steady state as shown in the case study in [42]. Here, these constraints of the tie-line flows between the groups are not considered so as to minimize the control cost of the system.

We refer to level 1 for the coordination control of all groups, level 2 for the control of a group, and level 3 for the primary control of a node. MLPIAC focuses on the secondary frequency control at level 1 and 2.

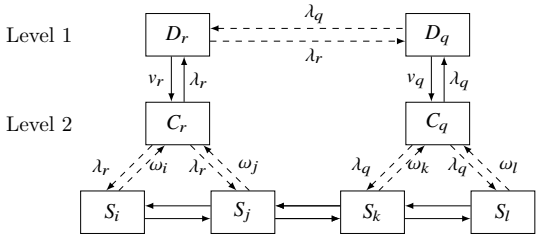

Fig. 1. Diagram of the multi-level control of power systems and dynamic data exchanges. All the dashed lines denote the communications between the controllers, the solid lines between the subsystems denote the physical coupling, and the solid lines between level 1 and level 2 denote the data exchanges which do not need any communications.

In the following two subsections, we define MLPIAC and analyze its properties during the transient phase and at the steady state.

A. Definition of MLPIAC

Definition 3.2 (MLPIAC): Consider a large-scale power system (1) with Assumption (2.2) and (2.4), which is partitioned as in (7). At level 2, the dynamic control law in group A_r is described by the equations

$$\dot{\eta}_r = \sum_{i\in\mathcal{V}_{M_r}\cup\mathcal{V}_{F_r}} D_i\omega_i + k_3 v_r, \tag{8a}$$

$$\dot{\xi}_r = -k_1\Big(\sum_{i\in\mathcal{V}_{M_r}} M_i\omega_i + \eta_r\Big) - k_2\xi_r, \tag{8b}$$

$$0 = \frac{\lambda_r}{\alpha_r} - k_2\xi_r, \tag{8c}$$

$$u_i = \frac{\lambda_r}{\alpha_i},\ i \in \mathcal{V}_{K_r}, \tag{8d}$$

$$\frac{1}{\alpha_r} = \sum_{i\in\mathcal{V}_{K_r}} \frac{1}{\alpha_i} \tag{8e}$$

where η_r, ξ_r are state variables of the group controller, v_r is an algebraic variable, $k_1, k_2, k_3 \in (0, \infty)$ are parameters, α_r is a constant defined as the control price of group A_r, u_i is the control input at node i in this group.

At level 1, the coordination for the group is an algebraic equation only

$$v_r = \sum_{q\in Z_m} l_{rq}(\lambda_r(t) - \lambda_q(t)) \tag{9}$$

where $\{\lambda_r(t),\ r \in Z_m\}$ are inputs and $\{v_r(t),\ r \in Z_m\}$ are outputs of the coordinators, $l_{rq} \in [0, \infty)$ is the weight of the communication line connecting group A_r and A_q, which can be chosen to accelerate the consensus of the marginal costs. l_{rq} defines a weighted undirected communication network with Laplacian matrix $(L_{rq}) \in \mathbb{R}^{m\times m}$

$$L_{rq} = \begin{cases} -l_{rq}, & r \neq q, \\ \sum_{k\neq i} l_{rk}, & r = q, \end{cases} \tag{10}$$

This article has been accepted for publication in a future issue of this journal, but has not been fully edited. Content may change prior to final publication. Citation information: DOI 10.1109/TAC.2019.2934014, IEEE Transactions on Automatic Control

Fig. 1 illustrates the control architecture of MLPIAC. At level 2 the control task of each group controller is to restore the nominal frequency and minimize the local control cost in the groups by centralized control. Within group A_r, the group controller collects the frequency deviations $\{\omega_i,\ i \in \mathcal{V}_{M_r} \cup \mathcal{V}_{F_r}\}$ from the local nodes and calculates the marginal cost of the group λ_r with the algebraic value of v_r for the local nodes which further calculate $\{u_i,\ i \in \mathcal{V}_{K_r}\}$ by (8d). The total control input of group A_r is denoted by $u_r = k_2\xi_r$. Rely 3.3 The requirement at this level includes the frequency measurement at the local nodes $\mathcal{V}_M \cup \mathcal{V}_F$ which can be satisfied in secondary frequency control, and the communications of the frequency deviations and the marginal costs between the local nodes and the group controller, which can be satisfied by the communication network as in Assumption (2.4).

At level 1 the control task is to reduce the overall control cost through coordination of the group marginal costs by distributed control. As shown in Fig. 1, the group controller of group r exchanges the marginal cost with its neighbors and calculates v_r in order to achieve a consensus which is a necessary condition for the economic power dispatch as stated in (5). The communicated data in this level are the group marginal costs between the group controllers. The requirement of these communications can also be satisfied by the communication network as in Assumption (2.4).

In MLPIAC, the communicated data also include the moment inertia, the droop control coefficients and the control prices at the local nodes in a group, which are static data and are not necesary to communicate as frequently as the dynamic data as shown in Fig. 1

MLPIAC can also be implemented in an area of the multi-area control where the area is partitioned into such high level groups that cooperate to minimize the control cost.

MLPIAC has two special cases. (1) If each group consists of a single node, MLPIAC reduces to a distributed control law, which is named *Distributed Power-Imbalance Allocation Control* (DPIAC) and has the following form

$$\dot{\eta}_i = D_i\omega_i + k_3\sum_{j\in\mathcal{V}} l_{ij}(k_2\alpha_i\xi_i - k_2\alpha_j\xi_j), \tag{11a}$$

$$\dot{\xi}_i = -k_1(M_i\omega_i + \eta_i) - k_2\xi_i, \tag{11b}$$

$$u_i = k_2\xi_i. \tag{11c}$$

(2) If the entire network is controlled as a single group, then it reduces to a centralized control law named *Gather-Broadcast Power-Imbalance Allocation Control* (GBPIAC), which is described by

$$\dot{\eta}_s = \sum_{i\in\mathcal{V}_F} D_i\omega_i, \tag{12a}$$

$$\dot{\xi}_s = -k_1(\sum_{i\in\mathcal{V}_M} M_i\omega_i + \eta_s) - k_2\xi_s, \tag{12b}$$

$$u_i = \frac{\alpha_s}{\alpha_i}k_2\xi_s,\ i \in \mathcal{V}_K, \tag{12c}$$

$$\frac{1}{\alpha_s} = \sum_{i\in\mathcal{V}_K}\frac{1}{\alpha_i}, \tag{12d}$$

where $\eta_s,\ \xi_s$ are state variables of the central controller. In the next subsection, it will be shown that MLPIAC includes a trade-off between DPIAC and GBPIAC.

B. Properties of MLPIAC

In this section, we analyse the properties of MLPIAC in the transient phase and steady state and verify whether it solves Problem 2.3. The following proposition describes the properties of MLPIAC during the transient phase.

Proposition 3.3: Consider a large-scale power system partitioned as in (7), MLPIAC has the following properties during the transient phase,

(a) at any time $t \in T$, the total control input u_s of the system satisfies,

$$\dot{\upsilon}_s = P_s + u_s, \tag{13a}$$

$$\dot{u}_s = -k_2\big(k_1\upsilon_s + u_s\big), \tag{13b}$$

where υ_s is an auxiliary variable. Furthermore, u_s converges to $-P_s$ directly without any extra oscillations if $k_2 \geq 4k_1$;

(b) at any time $t \in T$, within a group A_r, the inputs $\{u_i,\ i \in \mathcal{V}_{K_r}\}$ of the local controllers solve the following economic power dispatch problem

$$\min_{\{u_i\in\mathbb{R}, i\in\mathcal{V}_{K_r}\}} \sum_{i\in\mathcal{V}_{K_r}} \frac{1}{2}\alpha_i u_i^2 \tag{14}$$
$$s.t.\quad -u_r(t) + \sum_{i\in\mathcal{V}_{K_r}} u_i(t) = 0.$$

Proof: (a) Because of the symmetry of the matrix (L_{rq}), we derive from (9) that,

$$\sum_{r\in Z_m} v_r = \sum_{r,q\in Z_m} l_{rq}(\lambda_r - \lambda_q) = 0. \tag{15}$$

Summing all the equations in (1), we obtain

$$\sum_{i\in\mathcal{V}_M} M_i\dot{\omega}_i \quad = P_s - \textstyle\sum_{i\in\mathcal{V}_M\cup\mathcal{V}_F} D_i\omega_i + u_s. \tag{16}$$

Summing all the control inputs $\{u_r,\ r \in Z_m\}$ with $u_r = k_2\xi_r$, we derive the total control input of the system as $u_s = \sum_{r\in Z_m} k_2\xi_r$. It follows from (15) and (8b) that

$$\dot{u}_s(t) = -k_2\Big(k_1(\sum_{i\in\mathcal{V}_M} M_i\omega_i + \eta_s) + u_s(t)\Big), \tag{17}$$

where $\eta_s = \sum_{r\in Z_m}\eta_r$ and following (8a) with derivative

$$\dot{\eta}_s = \sum_{i\in\mathcal{V}_M\cup\mathcal{V}_F} D_i\omega_i \tag{18}$$

Let $\upsilon_s(t) = \sum_{i\in\mathcal{V}_M} M_i\omega_i + \eta_s$, we derive (13a) from (16) and (18), and (13b) from (17). Hence u_s satisfies (13). The eigenvalues of the system (13) are

$$\mu = \frac{-k_2 \pm \sqrt{k_2^2 - 4k_1k_2}}{2}. \tag{19}$$

To avoid the extra oscillation caused by the oscillations of u_s, the second-order system (13) should be over-damped or critical-damped, thus the eigenvalues in (19) must be real. This needs $k_2 \geq 4k_1$. Hence if $k_2 \geq 4k_1$, u_s converges to $-P_s$

This article has been accepted for publication in a future issue of this journal, but has not been fully edited. Content may change prior to final publication. Citation information: DOI 10.1109/TAC.2019.2934014, IEEE Transactions on Automatic Control

directly without any extra oscillations.
(b) Following (8d), we derive that at any time $t \in T$,

$$\alpha_i u_i = \alpha_j u_j = \alpha_r k_2 \xi_r, i, j \in \mathcal{V}_{K_r}.$$

So the necessary condition (5) for the optimization problem (14) is satisfied. Furthermore, with $\sum_{i\in\mathcal{V}_{K_r}} u_i(t) = u_r(t)$, the optimization problem (14) is solved at any time t. □

Remark 3.4: We use u_s to estimate the power-imbalance $-P_s$ in system (13) which can be seen as an observer of $-P_s$. Similar to the high gain observer [14], there may be overshoot in the initialization of the controllers due to the initial condition of the state. To the best of our knowledge, there do not seem general sufficient conditions on the system which guarantee that for all initial conditions the behavior of every state component is free of zero crossings and further eliminate this kind of overshoot. In this paper, we treat the case where the frequency trajectory fluctuates regularly and analyse the overshoots of u_s caused by those fluctuations.

The marginal costs $\{\lambda_r, A_r \subset A\}$ of the groups are different during the transient phase, which will achieve a consensus due to the principle of consensus control. The consensus speed of these marginal costs and the convergence speed of u_s determine convergence of the control cost to its optimal solution. Because one objective of Problem 2.3 is to eliminate the extra frequency oscillation, we set $k_2 \geq 4k_1$ in this paper.

Remark 3.5: In PIAC, the total control input satisfies

$$\dot{u}_s = -k(P_s + u_s).$$

Comparison with this total control input of PIAC, it can be easily deduced in (13) that one more state variable υ_s is introduced. The motivation of this introduction is to realize the distributed control in which the consensus of the marginal costs can be accelerated by tuning the control coefficient k_3, which further decreases the control cost.

In order to further investigate how MLPIAC improves the transient performance of the frequency and marginal cost, we decompose the dynamics of the power system into the following four subprocesses.

(i) the convergence of u_s to $-P_s$ as in (13) with a speed determined by k_1,
(ii) the synchronization of the frequency deviation $\omega_i(t)$ to $\omega_s(t)$ which is a physical characteristic of the power system (1), and the synchronization speed is determined by $\{u_i(t),\ i \in \mathcal{V}_\mathcal{K}\}$ and $\{D_i,\ i \in \mathcal{V}_M \cup \mathcal{V}_F\}$;
(iii) the convergence of ω_s to ω_{syn} which further converges to zero as $u_s(t)$ converges to $-P_s$. This can be directly obtained from (3);
(iv) the consensus of the marginal costs $\{\lambda_r, A_r \subset A\}$ with a consensus speed determined by k_3 and (L_{ij}).

In GBPIAC, because the economic power dispatch problem is solved in a centralized way, the marginal costs of all nodes are identical.

In MLPIAC, the transient performance of the frequency oscillation and marginal costs can be improved by tuning the corresponding coefficients of the four subprocesses. The convergence of ω_{syn} to zero can be accelerated by a fast convergence of u_s, which can be obtained with a large k_1. The synchronization process of ω_i can be improved by tuning $\{D_i,\ i \in \mathcal{V}_K\}$ which is the task of primary control. The corresponding actuators includes *Power System Stabilizer* (PSS) systems embedded in the damping systems of the synchronous machines [19]. The parameter D_i can be set as in [8] or [21] focusing on the control cost optimality and the small signal stability respectively. The convergence of $\{u_i,\ i \in \mathcal{V}_K\}$ to their optimal solution can be improved by tuning k_3 or by a well designed (L_{rq}).

Furthermore, for a system with multiple groups, the size of the communication network with Laplacian matrix (L_{rq}) is much smaller than the one in DPIAC, the speed of achieving a consensus marginal cost of the groups is much faster in MLPIAC due to a larger second smallest eigenvalue of (L_{rq}) [33, chapter 4], and the number of nodes in each group is smaller than the total number of nodes, the communication and computations of each group controller is reduced.

Before introducing Proposition 3.7 which describes the properties of the steady state of the power system controlled by MLPIAC, we introduce the closed-loop system as follows.

$$\dot{\theta}_i = \omega_i, i \in \mathcal{V}_M \cup \mathcal{V}_F, \tag{20a}$$

$$M_i\dot{\omega}_i = P_i - D_i\omega_i - \sum_{j\in\mathcal{V}} B_{ij}\sin\theta_{ij} + \frac{\alpha_r}{\alpha_i}k_2\xi_r, i \in \mathcal{V}_{M_r} \subset \mathcal{V}_M, \tag{20b}$$

$$0 = P_i - D_i\omega_i - \sum_{j\in\mathcal{V}} B_{ij}\sin\theta_{ij} + \frac{\alpha_r}{\alpha_i}k_2\xi_r, i \in \mathcal{V}_{Fr} \subset \mathcal{V}_F, \tag{20c}$$

$$0 = P_i - \sum_{j\in\mathcal{V}} B_{ij}\sin\theta_{ij}, i \in \mathcal{V}_P, \tag{20d}$$

$$\dot{\eta}_r = \sum_{i\in\mathcal{V}_{M_r}\cup\mathcal{V}_{F_r}} D_i\omega_i + k_2k_3\sum_{q\in Z_m} l_{rq}(\alpha_r\xi_r - \alpha_q\xi_q), r \in Z_m, \tag{20e}$$

$$\dot{\xi}_r = -k_1(\sum_{i\in\mathcal{V}_{M_r}} M_i\omega_i + \eta_r) - k_2\xi_r,\ r \in Z_m \tag{20f}$$

where $\theta_{ij} = \theta_i - \theta_j$ for $(i, j) \in \mathcal{E}$, i and j are the node indices, and r, q are the group indices.

As in the Kuramoto-model [6], the closed-loop system (20) may not have a synchronous state if the power injections $\{P_i, \in \mathcal{V}\}$ are much larger that the line capacity $\{B_{ij}, (i, j) \in \mathcal{E}\}$ [8] and [39]. We assume there exists a synchronous state for the power system, which can be satisfied by reserving some margin in the line capacity by tertiary control.

Assumption 3.6: There exists a synchronous state for the closed-loop system (20) such that

$$\theta^* \in \Theta = \left\{\theta_i \in \mathbb{R},\ \forall i \in \mathcal{V} \middle| |\theta_i - \theta_j| < \frac{\pi}{2}, \forall (i, j) \in \mathcal{E}\right\}$$

where $\theta^* = \mathrm{col}(\theta_i^*) \in \mathbb{R}^{n_t}$, n_t is the total number of nodes in $\mathcal{V}$. The condition $\theta^* \in \Theta$ is commonly referred to as a security constraint [23] and restricts the equilibrium to desired power flows.

Note that the equilibria with θ outside Θ usually leads to undesired power flows which either have cyclic power flows or are unstable [39].

For the synchronous state of the closed-loop system, we have the following proposition.

Proposition 3.7: If the assumptions (2.2), (2.4) and (3.6)

This article has been accepted for publication in a future issue of this journal, but has not been fully edited. Content may change prior to final publication. Citation information: DOI 10.1109/TAC.2019.2934014, IEEE Transactions on Automatic Control

hold, then there exists at most one synchronous state for the closed-loop system (20) such that

$$\theta_i^* \in \Theta,\ i \in \mathcal{V} \tag{21a}$$
$$\omega_i^* = 0, \mathcal{V}_M \cup \mathcal{V}_F, \tag{21b}$$
$$P_s + k_2 \sum_{r\in Z_m} \xi_r^* = 0, \tag{21c}$$
$$k_1\eta_r^* + k_2\xi_r^* = 0,\ r \in Z_m, \tag{21d}$$
$$\alpha_r\xi_r^* - \alpha_q\xi_q^* = 0,\ \forall\ r, q \in Z_m, \tag{21e}$$
$$\alpha_i u_i^* - k_2\alpha_r\xi_r^* = 0,\ i \in \mathcal{V}_{K_r} \subset \mathcal{V}_K. \tag{21f}$$

Proof: From Proposition 3.3, the dynamics of u_s satisfies (13), which yields that $u_s^* = -P_s$ at the synchronous state. Thus (21c) is derived with $u_s(t) = \sum_{r\in Z_m} k_2\xi_r(t)$. Following (3), we further derive that $\omega_{syn} = 0$, which yields (21b) with the definition of the synchronous state (2). By (20f), $\omega_i^* = 0$ and $\dot{\xi}_i^* = 0$ for all $i \in \mathcal{V}_K$, we derive (21d). By (20e) and $\omega_i^* = 0$, we obtain (21e). By (8c) and (8d), we arrive at (21f). From (21e,21f) it follows that $\alpha_i u_i^* = \alpha_j u_j^*$ for all $i, j \in \mathcal{V}_K$, thus the necessary condition (5) is satisfied. Following (21c), it yields $P + \sum_{i\in\mathcal{V}_K} u_i^* = 0$ and the economic dispatch problem (4) is solved subsequently. Accoding to [2], [29], there exists at most one synchronous state such that $\theta^* \in \Theta$. □

With the improved transient performance as stated in the dynamics decomposition and the properties of the system at the steady state as in Proposition 3.7, Problem 2.3 is solved.

Remark 3.8: MLPIAC actually includes proportional and integral control input, which are the terms $k_1 \sum_{i\in\mathcal{V}_{M_r}} M_i\omega_i$ and $k_1\eta_r$ respectively in (8b). In order to get a desired performance, the parameters M_i and D_i should be known. In practice, they are known for traditional synchronous machines [15]. However, they may not be known for the frequency dependent nodes. In that case, the uncertainties from these parameters can be added to the power-imbalance, which becomes a time-varying value and can be compensated by the controllers at the steady state because of the included integral control input. Theoretical analysis on the robustness of MLPIAC with these uncertainties needs to be further studied.

Remark 3.9: Through eigenvalue analysis or $\mathcal{H}_2/\mathcal{H}_\infty$ norm optimization, the existing control laws, e.g., the robust PI control in [5], the distributed averaging PI control [8], [1], and the distributed control law in [37], may also obtain the desired transient performance as that of MLPIAC. However, intensive computations are needed and the mechanism to improve the transient performance is not as clear as in MLPIAC. In addition, the multi-level control structure of MLPIAC has not been considered in these methods.

IV. Stability analysis of MLPIAC

In Proposition 2.3, we have proven that the total control input converges to the power-imbalance directly when $k_2 \geq 4k_1$, which does not imply the state of the power system converges to its steady state. In this section, we focus on the asymptotic stability of MLPIAC.

The power flows $\{B_{ij}\sin(\theta_{ij}), (i,j) \in \mathcal{E}\}$ only depend on the angle differences. As in [40], we choose a reference angle, e.g., $\theta_1 \in \mathcal{V}_M$, and transform the system state into a new coordinate system such that

$$\varphi_i = \theta_i - \theta_1,\ i \in \mathcal{V}.$$

which yields $\dot{\varphi}_i = \omega_i - \omega_1$ for all i in $\mathcal{V}_M \cup \mathcal{V}_F$. In the new coordinate, the closed-loop system (20) becomes

$$\dot{\varphi}_i = \omega_i - \omega_1, i \in \mathcal{V}_M \cup \mathcal{V}_F, \tag{22a}$$
$$M_i\dot{\omega}_i = P_i - D_i\omega_i - \sum_{j\in\mathcal{V}} B_{ij}\sin\varphi_{ij} + \frac{\alpha_r}{\alpha_i}k_2\xi_r,\ i \in \mathcal{V}_M, \tag{22b}$$
$$D_i\dot{\varphi}_i = P_i - D_i\omega_1 - \sum_{j\in\mathcal{V}} B_{ij}\sin\varphi_{ij} + \frac{\alpha_r}{\alpha_i}k_2\xi_r,\ i \in \mathcal{V}_F, \tag{22c}$$
$$0 = P_i - \sum_{j\in\mathcal{V}} B_{ij}\sin\varphi_{ij},\ i \in \mathcal{V}_P, \tag{22d}$$
$$\dot{\eta}_r = \sum_{i\in\mathcal{V}_{M_r}\cup\mathcal{V}_{F_r}} D_i\omega_i + k_2k_3 \sum_{q\in Z_m} l_{rq}(\alpha_r\xi_r - \alpha_q\xi_q),\ r \in Z_m, \tag{22e}$$
$$\dot{\xi}_r = -k_1\Big(\sum_{i\in\mathcal{V}_{M_r}} M_i\omega_i + \eta_r\Big) - k_2\xi_r,\ r \in Z_m \tag{22f}$$

which can be written in the form of DAEs (67) of Appendix B. Following Assumption (3.6), $\varphi = \mathrm{col}(\varphi_i) \in \mathbb{R}^{n_t}$ satisfies

$$\varphi \in \Phi = \Big\{\varphi_i \in \mathbb{R}, i \in \mathcal{V} || \varphi_i - \varphi_j| \leq \frac{\pi}{2}, \forall (i,j) \in \mathcal{E},\ \varphi_1 = 0\Big\}.$$

We make the following assumption that the control gain coefficients k_1, k_2, k_3 satisfy a certain condition (that will be proven to be a sufficient condition of the asymptotic stability of MLPIAC).

Assumption 4.1: Assume the control gain coefficients, k_1, k_2, k_3, satisfy that

$$\frac{k_2}{k_1} > \frac{2(\alpha D)_{\max}}{(\alpha D)_{\min}(1 + 2k_3\lambda_{\min})}$$

where $(\alpha D)_{\min} = \min\{\alpha_i D_i,\ i \in \mathcal{V}_K\}$, $(\alpha D)_{\max} = \max\{\alpha_i D_i,\ i \in \mathcal{V}_K\}$ and $\lambda_{\min}$ is the smallest nonzero eigenvalue of matrix $L\alpha_R$ where $L = (L_{rq}) \in \mathbb{R}^{m\times m}$ is defined in (10) and $\alpha_R = \mathrm{diag}(\alpha_r) \in \mathbb{R}^{m\times m}$.

We rewrite the state and algebraic variables into a vector form, $(\varphi, \omega, \eta, \xi) \in \mathbb{R}^{n_t} \times \mathbb{R}^n \times \mathbb{R}^m \times \mathbb{R}^m$. The following theorem states the asymptotic stability of the equilibrium of MLPIAC.

Theorem 4.2: If assumptions (2.2,2.4,3.6) and (4.1) hold, then for the closed-loop system (20),

(a) there exists an unique synchronous state $z^* = (\varphi^*, \omega^*, \eta^*, \xi^*) \in \Psi$ where $\Psi = \Phi \times \mathbb{R}^n \times \mathbb{R}^m \times \mathbb{R}^m$.
(b) there exists a domain $\Psi^d \subset \Psi$ such that starting at any initial state $z^0 = (\varphi^0, \omega^0, \eta^0, \xi^0) \in \Psi^d$ which satisfies the algebraic equations (22d), the state trajectory converges to the unique synchronous state $z^* \in \Psi$.

Remark 4.3: In MLPIAC, Assumptions (2.2, 2.4, 3.6) and (4.1) are both necessary and realistic at the same time. Assumptions (2.2) and (2.4) are necessary for the implementation of MLPIAC to solve the economic power dispatch problem (4). Assumptions (3.6) and (4.1) are general sufficient conditions for the stability of MLPIAC. Assumption (2.2) and (3.6) can be guaranteed by tertiary control and Assumption (2.4) by an effective communication infrastructure.

Remark 4.4: The inverse of damping coefficient, $\frac{1}{D_i}$ can be viewed as the control cost of primary control [8]. When

This article has been accepted for publication in a future issue of this journal, but has not been fully edited. Content may change prior to final publication. Citation information: DOI 10.1109/TAC.2019.2934014, IEEE Transactions on Automatic Control

$\alpha = \gamma D^{-1}$, $\gamma \in \mathbb{R}$ is a positive number, which indicates that the cost of the secondary frequency control is proportional to the primary control cost and leads to $(\alpha D)_{\min} = (\alpha D)_{\max}$, DPIAC is asymptotically stable if $k_2 > 2k_1$. Specially, Assumption (4.1) can be dropped in GBPIAC in the theoretical analysis as will be explained in Remark (4.7). For DPIAC and MLPIAC, our numerical simulations have shown that the control law is asymptotically stable though assumption (4.1) is not satisfied, which will be shown in section V.

In the following, we will prove Theorem (4.2). The closed-loop system (22) is rewritten in a vector form as follows,

$$\dot{\tilde{\varphi}} = \omega - \omega_1 1_n, \tag{23a}$$
$$M\dot{\omega} = P - D\omega - P^t + k_2\alpha^{-1}R\alpha_R\xi, \tag{23b}$$
$$0 = \tilde{P} - \tilde{P}^t, \tag{23c}$$
$$\dot{\eta} = R^T D\omega + k_2k_3L\alpha_R\xi, \tag{23d}$$
$$\dot{\xi} = -k_1(R^T M\omega + \eta) - k_2\xi, \tag{23e}$$

where $\tilde{\varphi} = \mathrm{col}(\varphi_i)$ with $i \in \mathcal{V}_M \cup \mathcal{V}_F$, $P = \mathrm{col}(P_i) \in \mathbb{R}^n$ for $i \in \mathcal{V}_M \cup \mathcal{V}_F$, $\tilde{P} = \mathrm{col}(P_j) \in \mathbb{R}^{n_p}$ for $j \in \mathcal{V}_P$, $P^t = \mathrm{col}(P_i^t) \in \mathbb{R}^n$ with $P_i^t = \sum_{j\in\mathcal{V}} B_{ij}\sin\varphi_{ij}$ for $i \in \mathcal{V}_M \cup \mathcal{V}_F$, $\tilde{P}^t = \mathrm{col}(\tilde{P}_i^t) \in \mathbb{R}^{n_p}$ with $\tilde{P}_i^t = \sum_{j\in\mathcal{V}} B_{ij}\sin\varphi_{ij}$ for $i \in \mathcal{V}_P$. Note that $\tilde{\varphi}$ only includes the variables $\{\varphi_i, i \in \mathcal{V}_M \cup \mathcal{V}_F\}$ while φ includes $\{\varphi_i, i \in \mathcal{V}\}$. For the definitions of M, D, R, α_R, we refer to Appendix A.

We transform the state of the control law (23d,23e) to a new coordinate as a preparation for the stability analysis of MLPIAC. Following Theorem C.2 in Appendix C, let $\rho = Q^{-1}\eta$ and $\sigma = Q^{-1}\xi$. The vector form (23d,23e) becomes

$$\dot{\rho} = Q^{-1}R^T D\omega + k_2k_3\Lambda\sigma,$$
$$\dot{\sigma} = -k_1Q^{-1}R^T M\omega - k_1\rho - k_2\sigma,$$

where all the components $(\rho_i,\ \sigma_i)$ of $(\rho,\ \sigma)$ are decoupled from each other. When writing the dynamics of $(\rho_i,\ \sigma_i)$ separately, we derive

$$\dot{\rho}_i = Q_{vi}^T R^T D\omega + k_2k_3\lambda_i\sigma_i, \tag{25a}$$
$$\dot{\sigma}_i = -k_1Q_{vi}^T R^T M\omega - k_1\rho_i - k_2\sigma_i, \tag{25b}$$

where Q^{-1} is decomposed into vectors, i.e., $Q^{-1} = (Q_{v1}, Q_{v2}, \cdots, Q_{vn})$. In (25), the controller of component i calculates the output σ_i with the input ω for the power system. We investigate the dynamic behavior of the component (ρ_1, σ_1) and $\{(\rho_i, \sigma_i),\ i = 2, \cdots, n\}$ of (ρ, σ) respectively.

For the first component (ρ_1, σ_1) of (ρ, σ), we have the following lemma.

Lemma 4.5: The dynamics of (ρ_1, σ_1) described by (25) is identical to that of (η_s, ξ_s) in (12).

Proof: By (25) and (66b), $\lambda_1 = 0$ and $Q_{vi} = 1_m$ from (71a), we derive the dynamics of (ρ_1, σ_1) as follows

$$\dot{\rho}_1 = 1_m R^T D\omega = \sum_{i\in\mathcal{V}_M\cup\mathcal{V}_F} D_i\omega_i, \tag{26a}$$
$$\dot{\sigma}_1 = -k_1(1_m R^T M\omega + \rho_1) - k_2\sigma_1 \tag{26b}$$
$$= -k_1(\sum_{i\in\mathcal{V}_M} M_i\omega_i + \rho_1) - k_2\sigma_1. \tag{26c}$$

In addition, by summing all the equations in (23b) for all $i \in \mathcal{V}$, we derive

$$\begin{aligned}\sum_{i\in\mathcal{V}_M} M_i\dot{\omega}_i &= P_s - \sum_{i\in\mathcal{V}_M\cup\mathcal{V}_F} D_i\omega_i + k_2 1_n^T\alpha^{-1}R\alpha_R\xi \\ &\quad \text{by (66)} \\ &= P_s - \sum_{i\in\mathcal{V}_M\cup\mathcal{V}_F} D_i\omega_i + k_2 1_m^T\xi \\ &\quad \text{by (70a)} \\ &= P_s - \sum_{i\in\mathcal{V}_M\cup\mathcal{V}_F} D_i\omega_i + k_2\sigma_1. \end{aligned} \tag{27}$$

So $k_2\sigma_1$ is the control input for the power system (1) as $k_2\xi_s$. Furthermore, the initial values of (ρ_1, σ_1) and (η_s, ξ_s) are identical, which are both computed from $\{\omega_i(0), i \in \mathcal{V}_K\}$, so the dynamics of (ρ_1, σ_1) is identical to that of (η_s, ξ_s) in (12) if under the same initial values. □

As described in Remark 3.8, the total control ipnut of MLPIAC includes a proportional and an integral control input. With the superposition principle, we decompose the dynamics of (ρ_i, σ_i) for $i = 2, \cdots, m$ for the proportional and the integral input into the following two independent dynamics.

$$\dot{\rho}_{mi} = k_2k_3\lambda_i\sigma_{mi},$$
$$\dot{\sigma}_{mi} = -k_1Q_{vi}^T R^T M\omega - k_1\rho_{mi} - k_2\sigma_{mi},$$

and

$$\dot{\rho}_{di} = Q_{vi}^T R^T D\omega + k_2k_3\lambda_i\sigma_{di},$$
$$\dot{\sigma}_{di} = -k_1\rho_{di} - k_2\sigma_{di},$$

from which it can be easily derived that $\rho_i = \rho_{mi} + \rho_{di}$ and $\sigma_i = \sigma_{mi} + \sigma_{di}$.

In the coordinate of $(\varphi, \omega, \rho_1, \sigma_1, \rho_m, \sigma_m, \rho_d, \sigma_d)$, the closed-loop system (23) becomes

$$\dot{\tilde{\varphi}} = \omega - \omega_1 1_n, \tag{30a}$$
$$M\dot{\omega} = P - D\omega - P^t + k_2\alpha^{-1}R\alpha_R Q\sigma, \tag{30b}$$
$$0 = \tilde{P} - \tilde{P}^t, \tag{30c}$$
$$\dot{\rho}_1 = 1_m^T R^T D\omega, \tag{30d}$$
$$\dot{\sigma}_1 = -k_1 1_m^T R^T M\omega - k_1\rho_1 - k_2\sigma_1, \tag{30e}$$
$$\dot{\rho}_m = k_2k_3\Lambda\sigma_m, \tag{30f}$$
$$\dot{\sigma}_m = -k_1W^T R^T M\omega - k_1\rho_m - k_2\sigma_m, \tag{30g}$$
$$\dot{\rho}_d = W^T R^T D\omega + k_2k_3\Lambda\sigma_d, \tag{30h}$$
$$\dot{\sigma}_d = -k_1\rho_d - k_2\sigma_d, \tag{30i}$$

where $\sigma = \mathrm{col}(\rho_i)$, $\rho_i = \rho_{mi} + \rho_{di}$ for $i = 2, \cdots, m$, W is defined as in Theorem (C.2). Note that $\Lambda \in \mathbb{R}^{(m-1)\times(m-1)}$ only includes the nonzero eigenvalues of $L\alpha_R$, which is different from the one in Appendix A.

Following Proposition (3.7), for the closed-loop system (30) we have the following Lemma on the equilibrium state.

Lemma 4.6: In the coordinate of $(\varphi, \omega, \rho_1, \sigma_1, \rho_m, \sigma_m, \rho_d, \sigma_d)$, the unique equilibrium state $(\theta^*, \omega^*, \eta^*, \xi^*)$ of the closed-loop system (20) proposed in Proposition (3.7) is equivalent to $(\varphi^*, \omega^*, \rho_1^*, \sigma_1^*, \rho_m^*, \sigma_m^*, \rho_d^*, \sigma_d^*) \in \Phi \times \mathbb{R}^n \times \mathbb{R} \times \mathbb{R} \times \mathbb{R}^{m-1} \times$

This article has been accepted for publication in a future issue of this journal, but has not been fully edited. Content may change prior to final publication. Citation information: DOI 10.1109/TAC.2019.2934014, IEEE Transactions on Automatic Control

$\mathbb{R}^{m-1} \times \mathbb{R}^{m-1} \times \mathbb{R}^{m-1}$ such that

$$\varphi^* \in \Phi = \Big\{\varphi \in \mathbb{R}^{n_t} \,||\varphi_i - \varphi_j| < \frac{\pi}{2},\ \forall (i,j) \in \mathcal{E}, \varphi_1 = 0\Big\}, \tag{31a}$$

$$\omega_i^* = 0,\ i \in \mathcal{V}_M \cup \mathcal{V}_F, \tag{31b}$$

$$k_1\rho_1^* + k_2\sigma_1^* = 0, \tag{31c}$$

$$k_2\sigma_1^* + P_s = 0, \tag{31d}$$

$$\rho_{mi}^* = 0,\ i = 2, \cdots, n, \tag{31e}$$

$$\sigma_{mi}^* = 0,\ i = 2, \cdots, n, \tag{31f}$$

$$\rho_{di}^* = 0,\ i = 2, \cdots, n, \tag{31g}$$

$$\sigma_{di}^* = 0,\ i = 2, \cdots, n, \tag{31h}$$

Proof: When mapping θ to φ, we can easily obtain $\varphi \in \Phi = \Big\{\varphi \in \mathbb{R}^{n_t} \,||\varphi_i - \varphi_j| < \frac{\pi}{2},\ \forall (i,j) \in \mathcal{E}, \varphi_1 = 0\Big\}$, $\omega^* = 0$ can be directly derived from Proposition (3.7).

By Lemma (4.5), we have $(\rho_1^*, \sigma_1^*) = (\eta_s^*, \sigma_s^*)$ at the steady state, which yields (31c) and (31d).

By the dynamics (25) of (ρ_{mi}, σ_{mi}) and that of (ρ_{di}, σ_{di}), we derive that $(\rho_{mi}^*, \sigma_{mi}^*) = (0,0)$ and $(\rho_{di}^*, \sigma_{di}^*) = (0,0)$ for all $i = 2, \cdots, n$, at the steady state, which lead to (31e)-(31h). □

In order to prove the asymptotic stability of the equilibrium $(\theta^*, \omega^*, \eta^*, \xi^*)$, we only need to prove the asymptotic stability of the equilibrium $(\varphi^*, \omega^*, \rho_1^*, \sigma_1^*, \rho_m^*, \sigma_m^*, \rho_d^*, \sigma_d^*)$. We define function

$$U(\varphi) = \sum_{(i,j)\in\mathcal{E}} B_{ij}(1 - \cos(\varphi_i - \varphi_j)) \tag{32}$$

and variable $\upsilon_s = \sum_{i\in\mathcal{V}_M} M_i\omega_i + \rho_1$. By (27) and (26), we obtain dynamics of (υ_s, σ_1),

$$\dot{\upsilon}_s = P_s + k_2\sigma_1, \tag{33a}$$

$$\dot{\sigma}_1 = -k_1\upsilon_s - k_2\sigma_1, \tag{33b}$$

with equilibrium state $(\upsilon_s^*, \sigma_1^*) = (\frac{1}{k_1}P_s, -\frac{1}{k_2}P_s)$.

In the following, we prove the equilibrium $(\theta^*, \omega^*, \rho_1^*, \sigma_1^*, \rho_m^*, \sigma_m^*, \rho_d^*, \sigma_d^*)$. is locally asymptotically stable following Lyapunov method.

Proof of Theorem (4.2): The existence and uniqueness of the synchronous state in Ψ follows Proposition (3.7) directly. Since the closed-loop system (20) is equivalent to (30), we prove the equilibrium $(\varphi^*, \omega^*, \rho_1^*, \sigma_1^*, \rho_m^*, \sigma_m^*, \rho_d^*, \sigma_d^*)$ of (30) is locally asymptotically stable. The proof follows Theorem (B.3). It follows [40, Lemma 5.2] that the algebraic equations (22d) are regular. In addition, there exists an unique equilibrium for the closed-loop system (30) following Lemma (4.6), we only need to find a Lyapunov function $V(x, y)$ as in Theorem (B.3).

Before introducing the Lyapunov function candidate, we define the following functions.

$$V_0 = U(\varphi) - U(\varphi^*) - \nabla_\varphi U(\varphi^*)(\varphi - \varphi^*) + \frac{1}{2}\omega^T M\omega,$$

$$V_1 = (c_1+1)\Big(\frac{1}{2k_1}(k_1\upsilon_s - k_1\upsilon_s^*)^2 + \frac{1}{2k_2}(k_2\sigma_1 - k_2\sigma_1^*)^2\Big) + \frac{1}{2k_2}(k_2\sigma_1 - k_2\sigma_1^*)^2 + \frac{1}{2k_1}(k_1\upsilon_s + k_2\sigma_1)^2,$$

where $c_1 \in \mathbb{R}$ and $k_1\upsilon_s^* + k_2\sigma_1^* = 0$ has been used. Denote $x_m = k_1\rho_m$, $y_m = k_2\sigma_m$, $z_m = k_1\rho_m + k_2\sigma_m$, $x_d = k_1\rho_d$, $y_d = k_2\sigma_d$, $z_d = k_1\rho_d + k_2\sigma_d$ and define

$$V_m = \frac{\beta_m}{2}x_m^T C_m x_m + \frac{(1+\beta_m)k_1k_3}{2k_2}y_m^T C_m\Lambda y_m + \frac{1}{2}z_m^T C_m z_m,$$

$$V_d = \frac{\beta_d c_d}{2}x_d^T x_d + \frac{(1+\beta_d)c_d k_1 k_3}{2k_2}y_d^T\Lambda y_d + \frac{c_d}{2}z_d^T z_d,$$

where $\beta_m \in \mathbb{R}$, $\beta_d \in \mathbb{R}$, $c_d \in \mathbb{R}$ are positive and $C_m = \mathrm{diag}(c_{mi}) \in \mathbb{R}^{(m-1)\times(m-1)}$ with all the diagonal elements $c_{mi} > 0$, and $\Lambda \in \mathbb{R}^{(m-1)\times(m-1)}$ is a diagonal matrix with diagonal elements being the nonzero eigenvalues of $L\alpha_R$.

In the following, we focus on the derivatives of the functions V_0, V_1, V_m, V_d. The derivative of V_0 is

$$\begin{aligned}
\dot{V}_0 &= -\omega^T D\omega + (k_2\sigma - k_2\sigma^*)^T Q^T\alpha_R R^T\alpha^{-1}\omega \\
&\quad \text{by } Q = [Q_1, Q_2, \cdots, Q_n] \text{ and } S = [Q_2, \cdots, Q_n]. \\
&= -\omega^T D\omega + (k_2\sigma_1 - k_2\sigma_1^*)Q_1^T\alpha_R R^T\alpha^{-1}\omega \\
&\quad + (k_2\sigma - k_2\sigma^*)^T S^T\alpha_R R^T\alpha^{-1}\omega \\
&= -\omega^T D\omega + (k_2\sigma_1 - k_2\sigma_1^*)Q_1^T\alpha_R R^T\alpha^{-1}\omega \\
&\quad + (k_2\sigma_m - k_2\sigma_m^*)^T S^T\alpha_R R^T\alpha^{-1}\omega \\
&\quad + (k_2\sigma_d - k_2\sigma_d^*)^T S^T\alpha_R R^T\alpha^{-1}\omega, \\
&\quad \text{by } S^T\alpha_R = W^T,\ Q_1^T\alpha_R = Q_{v_1}^T,\ \sigma_m^* = 0 \\
&= -\omega^T D\omega + (k_2\sigma_1 - k_2\sigma_1^*)Q_{v_1}^T R^T\alpha^{-1}\omega \\
&\quad + (k_2\sigma_m)^T W^T R^T\alpha^{-1}\omega + (k_2\sigma_d)^T W^T R^T\alpha^{-1}\omega \\
&= -\omega^T D\omega + (k_2\sigma_1 - k_2\sigma_1^*)Q_{v_1}^T R^T\alpha^{-1}\omega \\
&\quad + y_m^T W^T R^T\alpha^{-1}\omega + y_d^T W^T R^T\alpha^{-1}\omega.
\end{aligned}$$

The derivative of V_1 can be rewritten by adding and subtracting a term

$$\begin{aligned}
\dot{V}_1 &= -(c_1+1)(k_2\sigma_1 - k_2\sigma_1^*)^2 - \frac{k_2}{k_1}(k_1\upsilon + k_2\sigma_1)^2 \\
&= -(k_2\sigma_1 - k_2\sigma_1^*)Q_{v1}^T R^T\alpha^{-1}\omega + (k_2\sigma_1 - k_2\sigma_1^*)Q_{v1}^T R^T\alpha^{-1}\omega \\
&\quad - (c_1+1)(k_2\sigma_1 - k_2\sigma_1^*)^2 - \frac{k_2}{k_1}(k_1\upsilon + k_2\sigma_1)^2.
\end{aligned}$$

By inequalities

$$\begin{aligned}
(k_2\sigma_1 - k_2\sigma_1^*)Q_{v1}^T R^T\alpha^{-1}\omega &\le \frac{1}{8}\omega^T\epsilon D\omega \\
&\quad + 2(k_2\sigma_1 - k_2\sigma_1^*)^2 Q_{v1}^T R^T\alpha^{-2}(\epsilon D)^{-1}RQ_{v1},
\end{aligned}$$

we obtain

$$\begin{aligned}
\dot{V}_1 &\le -(k_2\sigma_1 - k_2\sigma_1^*)Q_{v1}^T R^T\alpha^{-1}\omega + \frac{1}{8}\omega^T\epsilon D\omega \\
&\quad + 2(k_2\sigma_1 - k_2\sigma_1^*)^2 Q_{v1}^T R^T\alpha^{-2}(\epsilon D)^{-1}RQ_{v1} \\
&\quad - (c_1+1)(k_2\sigma_1 - k_2\sigma_1^*)^2 - \frac{k_2}{k_1}(k_1\upsilon_s + k_2\sigma_1)^2 \\
&\quad \text{let } c_1 = 2Q_{v1}^T R^T\alpha^{-2}(\epsilon D)^{-1}RQ_{v1} \\
&= -(k_2\sigma_1 - k_2\sigma_1^*)Q_{v1}^T R^T\alpha^{-1}\omega + \frac{1}{8}\omega^T\epsilon D\omega \\
&\quad - (k_2\sigma_1 - k_2\sigma_1^*)^2 - \frac{k_2}{k_1}(k_1\upsilon + k_2\sigma_1)^2.
\end{aligned}$$

The derivative of V_m is

$$\begin{aligned}
\dot{V}_m &= -k_2 z_m^T C_m z_m - \beta_m k_1 k_3 y_m^T C_m\Lambda y_m \\
&\quad - k_1 k_2 z_m^T C_m W^T R^T M\omega - (1+\beta_m)k_1^2 k_3 y_m^T C_m\Lambda W^T R^T M\omega
\end{aligned}$$

This article has been accepted for publication in a future issue of this journal, but has not been fully edited. Content may change prior to final publication. Citation information: DOI 10.1109/TAC.2019.2934014, IEEE Transactions on Automatic Control

$$
\begin{aligned}
&= -y_m^T W^T R^T \alpha^{-1}\omega + y_m^T W^T R^T \alpha^{-1}\omega - k_2 z_m^T C_m z_m \\
&\quad - \beta_m k_1 k_3 y_m^T C_m \Lambda y_m - k_1 k_2 z_m^T C_m W^T R^T M\omega \\
&\quad - (1+\beta_m) k_1^2 k_3 y_m^T C_m \Lambda W^T R^T M\omega \\
&= -y_m^T W^T R^T \alpha^{-1}\omega + \sum_{i=2}^{n} y_{mi} Q_{vi}^T R^T \alpha^{-1}\omega - k_2 \sum_{i=2}^{n} c_{mi} z_{mi}^2 \\
&\quad - \beta_m k_1 k_3 \sum_{i=2}^{n} c_{mi}\lambda_i y_{mi}^2 - k_1 k_2 \sum_{i=2}^{n} c_{mi} z_{mi} Q_{vi}^T R^T M\omega \\
&\quad - (1+\beta_m) k_1^2 k_3 \sum_{i=2}^{n} \Big(c_{mi}\lambda_i y_{mi} Q_{vi}^T R^T M\omega \Big) \\
&= -y_m^T W^T R^T \alpha^{-1}\omega - k_2 \sum_{i=2}^{n} c_{mi} z_{mi}^2 - \beta_m k_1 k_3 \sum_{i=2}^{n} c_{mi}\lambda_i y_m^2 \\
&\quad - k_1 k_2 \sum_{i=2}^{n} \Big(c_{mi} z_{mi} Q_{vi}^T R^T M\omega \Big) \\
&\quad + \sum_{i=2}^{n} y_{mi} \big(Q_{vi}^T R^T \alpha^{-1} - Q_{vi}^T (1+\beta_m) k_1^2 k_3 c_{mi}\lambda_i R^T M \big)\omega.
\end{aligned}
$$

By the following inequalities

$$
k_1 k_2 c_{mi} z_{mi} Q_{vi}^T R^T M\omega \le \frac{\omega^T \epsilon D \omega}{8(n-1)} + r_m z_{mi}^2,
$$

where $r_z = 2(n-1)(k_1 k_2 c_{mi})^2 Q_{vi}^T R^T (D\epsilon)^{-1} M^2 R Q_{vi}$, and

$$
y_{mi} Q_{vi}^T R^T \big(\alpha^{-1} - (1+\beta_m) k_1^2 k_3 c_{mi}\lambda_i M\big)\omega \le \frac{\omega^T \epsilon D \omega}{8(n-1)} + r_z y_{mi}^2,
$$

where

$$
r_y = 2(n-1) Q_{vi}^T R^T \big((\alpha^{-1} - (1+\beta_m) k_1^2 k_3 c_{mi}\lambda_i M)^2 (\epsilon D)^{-1} R Q_{vi},
$$

we obtain

$$
\begin{aligned}
\dot V_m \le & -y_m^T W^T R^T \alpha^{-1}\omega + \frac{1}{4}\omega^T \epsilon D \omega - \sum_{i=2}^{n} z_{mi}^2 (k_2 c_{mi} - r_z) \\
& - \sum_{i=2}^{n} y_{mi}^2 (\beta_m k_1 k_3 c_{mi}\lambda_i - r_y).
\end{aligned}
$$

The derivative of V_d is

$$
\begin{aligned}
\dot V_d &= -c_d k_2 z_d^T z_d - y_d^T (c_d \beta_d k_1 k_3 \Lambda) y_d \\
&\quad + z_d^T ((1+\beta_d) c_d k_1) W^T R^T D\omega \\
&\quad - y_d^T (\beta_d c_d k_1 I_{n-1}) W^T R^T D\omega \\
&= -y_d^T W^T R^T \alpha^{-1}\omega + y_d^T W^T R^T \alpha^{-1}\omega - c_d k_2 z_d^T z_d \\
&\quad - y_d^T (c_d \beta_d k_1 k_3 \Lambda) y_d + z_d^T ((1+\beta_d) c_d k_1) W^T R^T D\omega \\
&\quad - y_d^T (\beta_d c_d k_1) W^T R^T D\omega \\
&= -y_d^T W^T R^T \alpha^{-1}\omega - c_d k_2 z_d^T z_d - y_d^T (c_d \beta_d k_1 k_3 \Lambda) y_d \\
&\quad + z_d^T ((1+\beta_d) c_d k_1) W^T R^T D\omega \\
&\quad + y_d^T W^T R^T (\alpha^{-1} - \beta_d c_d k_1 D)\omega.
\end{aligned}
$$

By $\lambda_{\min} \le \lambda_i$ for all $i = 2, \cdots, n$, and inequalities

$$
z_d^T W^T R^T ((1+\beta_d) c_d k_1) D\omega \le \frac{1}{2}\omega^T D \omega^T + \frac{1}{2} z_d^T X_z z_d,
$$

where $X_z = W^T R^T ((1+\beta_d) c_d k_1 D)^2 D^{-1} R W$, and

$$
y_d^T W^T R^T (\alpha^{-1} - \beta_d c_d k_1 D)\omega \le \frac{1}{2}\omega^T (D - \epsilon D)\omega + \frac{1}{2} y_d^T X_y y_d,
$$

where $X_y = W^T R^T (\alpha^{-1} - \beta_d c_d k_1 D)^2 (D - \epsilon D)^{-1} R W$, we derive,

$$
\begin{aligned}
\dot V_d &\le -y_d^T W^T R^T \alpha^{-1}\omega - c_d k_2 z_d^T z_d - c_d \beta_d k_1 k_3 \lambda_{\min} y_d^T y_d \\
&\quad + z_d^T W^T R^T ((1+\beta_d) c_d k_1) D\omega \\
&\quad + y_d^T W^T R^T (\alpha^{-1} - \beta_d c_d k_1 D)\omega \\
&\le -y_d^T W^T R^T \alpha^{-1}\omega + \omega^T D\omega - \frac{1}{2}\omega^T \epsilon D\omega \\
&\quad - z_d^T \big(c_d k_2 I_{m-1} - \frac{1}{2} X_z\big) z_d - y_d^T \big(c_d \beta_d k_1 k_3 \lambda_{\min} I_{m-1} - \frac{1}{2} X_y\big) y_d.
\end{aligned}
$$

We consider the following Lyapunov function candidate,

$$
V = V_0 + V_1 + V_m + V_d.
$$

In the following, we prove that (i) $\dot V \le 0$, (ii) equilibrium $z^* = (\varphi^*, \omega^*, \rho_1^*, \sigma_1^*, \rho_m^*, \sigma_m^*, \rho_d^*, \sigma_d^*)$ is a strict minimum of $V(\cdot)$ such that $\nabla V|_{z^*} = 0$ and $\nabla^2 V|_{z^*} > 0$, and (iii) z^* is the only isolated equilibrium in the invariant set $\{z \in \Phi \times \mathbb{R}^n \times \mathbb{R} \times \mathbb{R} \times \mathbb{R}^{m-1} \times \mathbb{R}^{m-1} \times \mathbb{R}^{m-1} \times \mathbb{R}^{m-1} | \dot V(z) = 0\}$ according to Theorem (B.3).

(i). V has derivative

$$
\dot V \le G_0 + G_1 + G_m + G_d, \tag{50}
$$

where the terms G_0, G_1, G_m, G_d are mainly from $\dot V_0, \dot V_1, \dot V_m, \dot V_d$ respectively by leaving the negative terms $-y_m^T W^T R^T \alpha^{-1}\omega$, $-y_d^T W^T R^T \alpha^{-1}\omega$. G_0, G_1, G_m, G_d have the following forms

$$
\begin{aligned}
G_0 &= -\frac{1}{8}\omega^T \epsilon D\omega, \\
G_1 &= -(k_2\sigma_1 - k_2\sigma_1^*)^2 - \frac{k_2}{k_1}(k_1\upsilon + k_2\sigma_1)^2, \\
G_m &= -\sum_{i=2}^{n} z_{mi}^2 (c_{mi} k_2 - r_z) - \sum_{i=2}^{n} y_{mi}^2 (\beta_m k_1 k_3 c_{mi}\lambda_i - r_y), \\
G_d &= -z_d^T (c_d k_2 I_{m-1} - \frac{1}{2} X_z) z_d - y_d^T (c_d \beta_d k_1 k_3 \lambda_{\min} I_{m-1} - \frac{1}{2} X_y) y_d.
\end{aligned}
$$

It is obvious that $G_0 \le 0$ and $G_1 \le 0$. In the following, we first focus on G_m. If there exist c_{mi} and β_m such that $c_{mi} k_2 - r_z > 0$ and $\beta_m k_1 k_3 c_{mi}\lambda_i - r_y > 0$, we have $G_m \le 0$ for all z_m and y_m. We verify that such c_{mi} and β_m do exist. By (66a) and (71b) in Appendix A and C, we have

$$
Q_{vi}^T R^T \alpha^{-1} R Q_{vi} = Q_{vi}^T \alpha_R^{-1} Q_{vi} = 1.
$$

So we only need to prove there exist c_{mi} and β_m such that

$$
\begin{aligned}
Q_{vi}^T R^T (c_{mi} k_2 \alpha^{-1}) R Q_{vi} - r_z > 0, \\
Q_{vi}^T R^T (\beta_m k_1 k_3 c_{mi}\lambda_i \alpha^{-1}) R Q_{vi} - r_y > 0,
\end{aligned}
$$

which yields

$$
c_{mi} k_2 \alpha^{-1} > 2(n-1)(c_{mi} k_1 k_2 M)^2 (\epsilon D)^{-1}, \tag{54a}
$$

$$
(\beta_m k_1 k_3 c_{mi}\lambda_i \alpha^{-1}) > 2(n-1)(\alpha^{-1} - c_{mi}(1+\beta_m) k_1 k_3 \lambda_i M)^2 (\epsilon D)^{-1}, \tag{54b}
$$

From (54), we derive

$$
c_{mi} I_{m-1} < \frac{\epsilon D}{2(n-1) k_1^2 k_2 M^2 \alpha},
$$

$$
\frac{I_{m-1}}{2a + b + \sqrt{4ab + b^2}} < c_{mi} I_{m-1} < \frac{2a + b + \sqrt{4ab + b^2}}{2a^2},
$$

where $a = (1+\beta_m) k_1^2 k_3 \lambda_i M\alpha)$, $b = \frac{\beta_m k_1 k_3 \alpha \lambda_i \epsilon D}{2(n-1)}$. There exists

This article has been accepted for publication in a future issue of this journal, but has not been fully edited. Content may change prior to final publication. Citation information: DOI 10.1109/TAC.2019.2934014, IEEE Transactions on Automatic Control

$c_{mi} > 0$ satisfying (54) if

$$\Big(\frac{I_{n-1}}{2a+b+\sqrt{4ab+b^2}}\Big)_{\max} < \Big(\frac{\epsilon D}{2(n-1)k_1^2k_2M^2\alpha}\Big)_{\min}$$

which can be satisfied by choosing a large β_m. This is because

$$\lim_{\beta_m\to\infty}\Big(\frac{1}{2a+b+\sqrt{4ab+b^2}}\Big)_{\max} = 0,$$

while the term $\Big(\frac{\epsilon D}{2(n-1)k_1^2k_2M^2\alpha}\Big)_{\min}$ does not depend on β_m. Hence there exist $c_{mi} > 0$ and $\beta_m > 0$ satisfying (54) and $G_m \le 0$ has been proven. Here $(\cdot)_{\max}$ and $(\cdot)_{\min}$ are as defined in Assumption (4.1).

In the following, we focus on G_d. If there exist c_d and β_d such that

$$c_dk_2I_{m-1} - \frac{1}{2}X_z > 0,$$
$$c_d\beta_dk_1k_3\lambda_{\min}I_{m-1} - \frac{1}{2}X_y > 0,$$

then $G_d \le 0$. We prove such c_d and β_d do exist with Assumption (4.1). By (66a) and (71b), we derive

$$W^TR^T\alpha^{-1}RW = W^T\alpha_R^{-1}W = I_{m-1}.$$

So we only need to prove there exist c_d and β_d such that

$$W^TR^T(c_dk_2\alpha^{-1})RW - \frac{1}{2}X_z > 0,$$
$$W^TR^T(c_d\beta_dk_1k_3\lambda_{\min})RW - \frac{1}{2}X_y > 0,$$

which yields

$$c_dk_2\alpha^{-1} > \frac{1}{2}(1+\beta_d)^2(c_dk_1D)^2D^{-1}, \tag{61a}$$
$$c_d\beta_dk_1k_3\lambda_{\min}\alpha^{-1} > \frac{1}{2}(\alpha^{-1}-\beta_dc_dk_1D)^2(D-\epsilon D)^{-1}. \tag{61b}$$

In the following, we prove that with assumption (4.1), there exist c_d and β_d satisfying the above two inequalities (61). We derive from (61) that

$$c_dI_{m-1} < \frac{2k_2}{(1+\beta_d)^2k_1^2\alpha D},$$
$$\frac{1}{\beta_dk_1\alpha Db_d} < c_dI_{m-1} < \frac{b_d}{\beta_dk_1\alpha D},$$

where

$$b_d = 1 + k_3\lambda_{\min}(1-\epsilon) + \sqrt{k_3^2\lambda_{\min}^2(1-\epsilon)^2 + 2k_3\lambda_{\min}(1-\epsilon)}.$$

There exists a c_d satisfying the two inequalities (61) if there exists a β_d such that

$$\frac{1}{\beta_dk_1(\alpha D)_{\min}b_d} < \frac{2k_2}{(1+\beta_d)^2k_1^2(\alpha D)_{\max}}. \tag{63}$$

Since

$$\lim_{\epsilon\to 0} b_d(\epsilon) = 1 + k_3\lambda_{\min} + \sqrt{k_3^2\lambda_{\min}^2 + 2k_3\lambda_{\min}} > 1 + 2k_3\lambda_{\min},$$

there exists a small $\epsilon > 0$ such that $b_d(\epsilon) > 1 + 2k_3\lambda_{\min}$. Subsequently (63) can be satisfied if

$$\frac{1}{\beta_dk_1(\alpha D)_{\min}(1+2k_3\lambda_{\min})} < \frac{2k_2}{(1+\beta_d)^2k_1^2(\alpha D)_{\max}}. \tag{65}$$

With assumption (4.1), we can obtain that there exist $\beta_d > 0$ satisfying (65). Hence $G_d < 0$ is proven and $\dot V \le 0$ subsequently.

(ii). We prove that the equilibrium z^* is a strict minimum of $V(\cdot)$. It can be easily verified that $V|_{z^*} = 0$ and

$$\nabla V|_{z^*} = \mathrm{col}(\nabla_\varphi V, \nabla_{\tilde z}V)|_{z^*} = 0,$$

where $\tilde z = (\omega, \rho_1-\rho_1^*, \sigma_1-\sigma_1^*, \rho_m, \sigma_m, \rho_d, \sigma_d)$. Here, we have used $(\omega^*, \rho_m^*, \sigma_m^*, \rho_d^*, \sigma_d^*) = 0$. The Hessian matrix of V at z^* is

$$\nabla^2V|_{z^*} = \mathrm{blkdiag}(L_p, H),$$

where bkldiag denotes a block diagonal matrix, L_p is Hessian matrix of V respect to φ with $\varphi_1 = 0$ and H is the Hessian matrix of V respect to $\tilde z$. It follows [40, Lemma 5.3] that L is positive definite. Since the components in V related to $\tilde z$ are all quadratic and positive definite, H is positive definite. Thus $\nabla^2V|_{z^*} > 0$.

(iii). The equilibrium is the only isolated one in the invariant set $\{(\varphi,\omega,\eta_m,\xi_m,\eta_d,\xi_d)|\dot V = 0\}$. Since $\dot V = 0$, it yields from (50) that $\tilde z = 0$. Hence φ_i are all constant. By Proposition (3.7), it follows that z^* is the only isolated equilibrium in the invariant set.

In this case, z^* is the only one equilibrium in the neighborhood of z^* such that $\Psi^d = \{(\varphi,\tilde z)|V(\varphi,\tilde z) \le c, \varphi \in \Phi\}$ for some $c > 0$. Hence with any initial state z^0 that satisfies the algebraic equations (22d), the trajectory converges to the equilibrium state z^*. □

Remark 4.7: In GBPIAC, the dynamics of $(\rho_m, \sigma_m, \rho_d, \sigma_d)$ vanish and the one of (ρ_1, σ_1) is left only. In the Lyapunov function $V(\cdot)$, with $V_m = 0$ and $V_d = 0$, it can be proven that the equilibrium of GBPIAC is locally asymptotically stable without Assumption (4.1).

V. Case Study

In this section, we evaluate the performance of MLPIAC on the IEEE-39 buses system as shown in Fig. 2. We compare MLPIAC to PIAC. For the comparison of PIAC to the traditional integral control laws, we refer to [42]. In order to study the trade-off between centralized and distributed control, we also compare MLPIAC with its two special cases, GBPIAC (12) and DPIAC (11). The performance of the subprocesses identified in Section III will be observed to study how the transient performance is improved in MLPIAC. The data of the test system are from [3]. The system consists of 10 generators, 39 buses, which serves a total load of about 6 GW. The voltage at each bus is constant which is derived by power flow calculation with the *Power System Analysis Toolbox* (PSAT) [19]. There are 49 nodes in the network including 10 nodes of generators and 39 nodes of buses. In order to involve the frequency dependent power sources, we change the buses which are not connected to synchronous machines into frequency dependent loads. Hence $\mathcal{V}_M = \{G1, G2, G3, G4, G5, G6, G7, G8, G9, G10\}$, $\mathcal{V}_P = \{30, 31, 32, 33, 34, 35, 36, 37, 38, 39\}$ and the other nodes are in set $\mathcal{V}_F$. The nodes in $\mathcal{V}_M \cup \mathcal{V}_F$ are all equipped with secondary frequency controllers such that $\mathcal{V}_K = \mathcal{V}_M \cup \mathcal{V}_F$. We remark

This article has been accepted for publication in a future issue of this journal, but has not been fully edited. Content may change prior to final publication. Citation information: DOI 10.1109/TAC.2019.2934014, IEEE Transactions on Automatic Control

that each synchronous machine is connected to a bus and its phase angle is rigidly tied to the rotor angle of the bus if the voltages of the system are constants [13]. Thus the angles of the synchronous machine and the bus have the same dynamics. The droop control coefficients are set to $D_i = 70$ (p.u./p.u. frequency deviation) for all $i \in \mathcal{V}_M \cup \mathcal{V}_F$ under the power base 100 MVA and frequency base 60 Hz. The setting of D_i leads to a frequency response of -1.2 p.u./0.1 Hz which equals to that of Quebec power grid connected by bus 39 [22]. The economic power dispatch coefficient $\alpha_i = 1/\beta_i$ where β_i is generated randomly with a uniform distribution on $(0, 1)$. In the simulations, the setting of $\{D_i,\ i \in \mathcal{V}_K\}$ and randomly generated coefficient $\{\alpha_i,\ i \in \mathcal{V}_K\}$ yield that $(\alpha D)_{\min} = 70$ and $(\alpha D)_{\max} = 42560$. The communication network is assumed to be a spanning tree network as shown by the red lines in Fig. 2, which satisfies the requirement in Assumption (2.4). For GBPIAC, the entire network is controlled as a single group. For DPIAC, each node $i \in \mathcal{V}_K$ is controlled as a single group. For MLPIAC, the network is divided into three groups by the dash-dotted black lines as shown in Fig. 2.

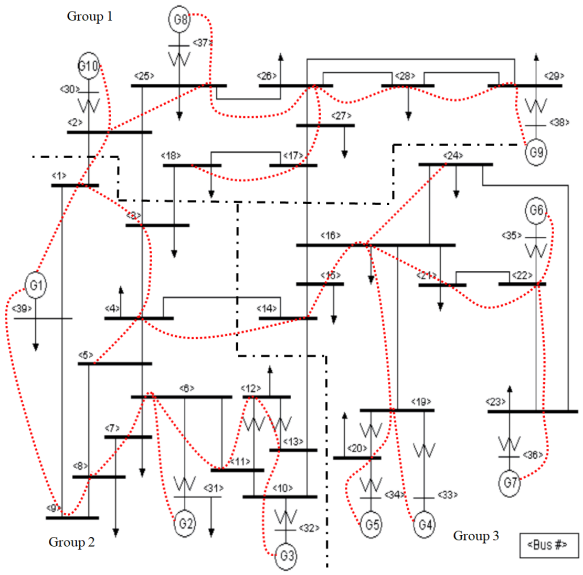

Fig. 2. IEEE New England test power system

We set $l_{ij} = 1$ if node i and j are connected by a communication line in DPIAC (11) and set $l_{rq} = 1$ if group r and q are connected by a communication line in MLPIAC (8). Note that group 1 and 2 are connected by communication line $(1, 2)$ and group 1 and 3 are connected by $(4, 14)$. However, group 1 and 3 are not connected by a communication line directly. So their marginal costs cannot be exchanged. With the control prices α and the Laplacian matrix of the communication network, it can be computed that $\lambda_{\min} = 0.0365$ for DPIAC and $\lambda_{\min} = 0.1933$ for MLPIAC.

At the beginning of the simulations, the power generation and loads are balanced with nominal frequency $f^* = 60$. At time $t = 5$ second, the loads at each of the buses 4, 12 and 20 increase by 66 MW step-wisely, which amounts to a total power imbalance of 198 MW and causes the frequency to drop below the nominal frequency.

We conduct the simulations with PSAT. The corresponding ordinary differential equations are discretized with the Euler-Forward method and the generated nonlinear system is solved with the Newton–Raphson method. Because the performance of PIAC has been compared with other control laws in [40], we compare the performance of the proposed MLPIAC law with PIAC only. For illustrations of the extra frequency oscillation caused by the overshoot of u_s, we refer to the simulations in, e.g., [8], [16], [30], [42], [43].

In the following, we evaluate the performance of the control approaches on restoring the nominal frequency with a minimized control cost. Because both GBPIAC and PIAC are centralized control laws, the principles of them on improving the transient performance are the same, i.e., tuning the corresponding gain coefficients in the decomposed first three sub-processes. Note that besides the three sub-processes shared with GBPIAC, i.e., the convergence processes of $u_s(t)$ to $-P_s$, $\omega_s(t)$ to zero, and the synchronization process of ω_i to $\omega_s(t)$, DPIAC considers the consensus process of the marginal costs of all the nodes and MLPIAC considers the consensus process of the marginal costs of all the groups. We consider the dynamics of the frequency $\overline{\omega}_i(t) = \omega_i(t) + f^*$ and abstract frequency $\overline{\omega}_s(t) = \omega_s(t) + f^*$ instead of $\omega_i(t)$ and $\omega_s(t)$ respectively. Here, the response of ω_s is obtained from (6) with u_s as the total control input of the three methods respectively.

The simulation results are shown in Fig. 3 where there are 20 plots in 5 rows and 4 columns. The plots in the rows from top to bottom illustrate the dynamics of the frequency $\overline{\omega}_i(t) \in \mathcal{V}_M$, control input $u_s(t)$, abstract frequency $\overline{\omega}_s(t)$, relative frequency $\omega_i(t) - \omega_s(t)$ for all $i \in \mathcal{V}_M$, and marginal costs of the controllers at the nodes of the synchronous machines in DPIAC and of the groups in MLPIAC, and the plots in the column from left to right illustrate the results of PIAC, GBPIAC, DPIAC with $k_3 = 10$, and MLPIAC with $k_3 = 10$ respectively. In these four simulations, we set $k = 0.4$ for PIAC, $k_1 = 0.4, k_2 = 1.6$ for GBPIAC, DPIAC and MLPIAC. Note that Assumption (4.1) is not satisfied in the simulations of DPIAC and MLPIAC, i.e., $\frac{k_2}{k_1} = 4$ while the values of $\frac{2(\alpha D)_{\max}}{(\alpha D)_{\min} + 2k_3\lambda_{\min}}$ are about 1203 and 1152 for DPIAC and MLPIAC with $k_3 = 10$ respectively. We remark that the relative frequency describes the synchronization process of $\omega_i(t)$ to $\omega_s(t)$, which is the main concern of primary control.

First focus attention on the response of the frequencies of the synchronous machines controlled by PIAC, GBPIAC, DPIAC and MLPIAC in Fig. $3(a_1 - a_4)$ and $3(c_1 - c_4)$. As the frequencies of PIAC, the frequencies of GBPIAC, DPIAC and MLPIAC are all restored to the nominal frequency, which indicates that DPIAC and MLPIAC are both asymptotically stable even though the assumption (4.1) is not satisfied. It can also be observed that the restorations of the frequencies do not introduce any extra oscillations. This is due the exponential convergence of the total control input to the power-imbalance without any overshoots as shown in Fig. $3(b_1 - b_4)$. With this exponentially convergence of the total control input, the abstract frequency is also restored to the nominal value

This article has been accepted for publication in a future issue of this journal, but has not been fully edited. Content may change prior to final publication. Citation information: DOI 10.1109/TAC.2019.2934014, IEEE Transactions on Automatic Control

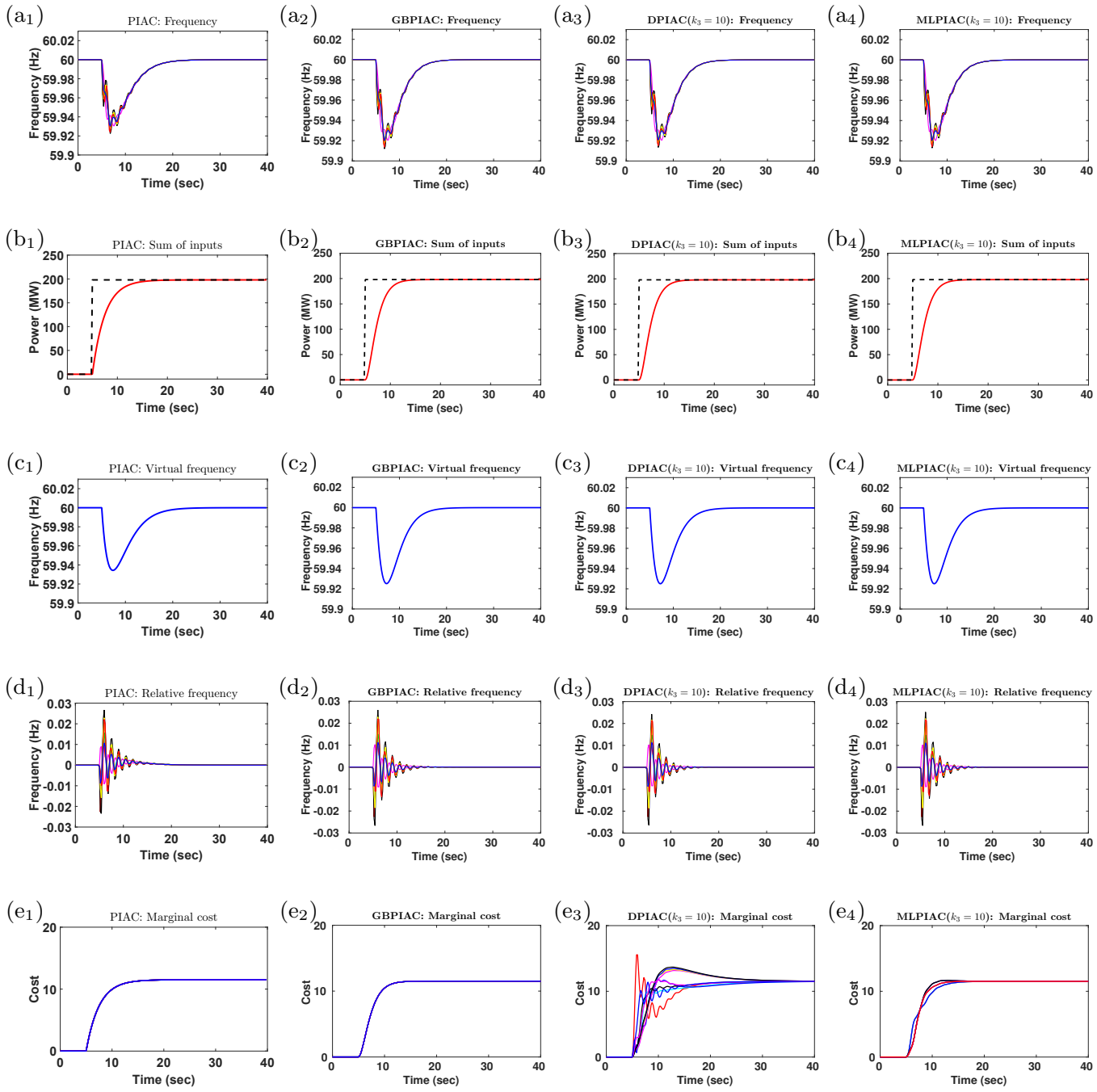

Fig. 3. The simulation results of the PIAC, GBPIAC, DPIAC and MLPIAC methods on IEEE 39-bus test system. The control coefficient is set $k = 0.4$ in PIAC, and $k_1 = 0.4, k_2 = 1.6$ in the other three methods. The black dashed lines in b_1-b_4, denote the power imbalance of the network.

directly. Since the droop coefficients are all identical in the four control laws, the synchronization of the frequencies to ω_s are similar which can observed in Fig. 3($d_1 - d_4$). Hence the frequency performances of the proposed control laws GBIAC, DPIAC and MLPIAC are similar to that of PIAC method. Thus, the transient performance of the frequency can also be improved by MLPIAC as PIAC as in the theoretical analysis.

Second, we turn to the responses of the marginal costs in Fig. 3($e_1 - e_4$). Because both PIAC and GBPIAC are centralized control, the marginal costs of them are all identical during the transient phase. In contrast, the marginal cost of DPIAC and MLPIAC are not identical during the transient phase but achieve a consensus at the steady state. The non-identical marginal costs during the transient phase in DPIAC and MLPIAC will lead to a higher control cost than in the centralized control. This illustrates the advantages of the centralized control compared with the distributed control on the minimization of the control cost. It can be easily imagined that as the scale of the network increases, the control burden of the central controller of GBPIAC on the computation and

This article has been accepted for publication in a future issue of this journal, but has not been fully edited. Content may change prior to final publication. Citation information: DOI 10.1109/TAC.2019.2934014, IEEE Transactions on Automatic Control

communication will increase, and the time for the marginal cost consensus in the pure distributed control DPIAC also increase, which further increases the control cost. These problems can be well addressed by MLPIAC. It can be easily verify in MLPIAC that the number of nodes in each group is much smaller than in GBPIAC, which decreases the control burden of the group controller. It can be observed in Fig. 3$(e_3 - e_4)$ that the differences of the marginal costs in MLPIAC are much smaller and the marginal costs achieve the consensus value at the steady state much faster than in DPIAC even though the control gain coefficient k_3 in these two methods are the same. This is because the Laplacian matrix (L_{rq}) of a smaller size communication network has a larger second smallest eigenvalue regardless to the line weights and the network topology, which leads to a faster consensus speed [33, chapter 4], and the size of the Laplacian matrix (L_{rq}) of MLPIAC in the simulations is 3 while the one of DPIAC is 39. Hence, for a large-scale network, *the multi-level control is more effective in decreasing the control cost than the distributed method.* This also indicates that MLPIAC balances the advantages and disadvantages of the centralized and distributed control.

VI. Conclusion

In this paper, we proposed a multi-level secondary frequency control, called *Multi-Level Power-Imbalance Allocation control* (MLPIAC), for a large-scale power system with multiple groups. Centralized control is implemented within each group and distributed control is implemented over the groups. At the steady state, the nominal frequency is restored with a minimized control cost. At the transient phase, the system performance can be improved by tuning the control gain coefficients without extensive computations. A trade-off between centralized control and distributed control is determined. The minimal cost can be more effectively achieved than by the purely distributed control due to the smaller number of groups than that of nodes in the network. The requirements on communications and computations are reduced compared to pure centralized control due to the smaller number of nodes in each group than that of nodes in the network.

However, Assumption (4.1) is still required for the asymptotic stability of MLPIAC even though it is not required in the numerical simulations. How to relax Assumption (4.1) theoretically still needs further consideration. The control law may be applicable for the power systems with general convex cost functions, which however needs further study specially in the asymptotic stability analysis. Furthermore, the communication network might not be reliable and there usually are time-delays and noises in the measurement of the frequency and communications in practice, in which case the robustness of MLPIAC needs to be evaluated.

Acknowledgment

The authors thank Dr. Johan L. A. Dubbeldam from Delft University of Technology, Prof. Tongchao Lu from Shandong University, Mr. César A. Uribe from University of Illinois for their useful discussions on this research, including the control algorithm synthesis and stability analysis.

Appendix A
Notations

Denote the number of nodes in the sets $\mathcal{V}_M, \mathcal{V}_F, \mathcal{V}_P$ and $\mathcal{V}_K$ by n_m, n_f, n_p, n respectively, the total number of nodes in the power system by n_t. So $n = n_m + n_f$ and $n_t = n_m + n_f + n_p$.

To express simply, we write a diagonal matrix $\beta = \text{diag}(\{\beta_i, i \cdots n\}) \in \mathbb{R}^{n\times n}$ with $\beta_i \in \mathbb{R}$ as $\text{diag}(\beta_i)$. It is convenient to introduce the matrices $D = \text{diag}(D_i) \in \mathbb{R}^{n\times n}$, $M = \text{diag}(M_i) \in \mathbb{R}^{n\times n}$, $\alpha = \text{diag}(\alpha_i) \in \mathbb{R}^{n\times n}$. Note that $M_i = 0$ for $i \in \mathcal{V}_F$ and $M_i > 0$ for $i \in \mathcal{V}_M$. Denote the identity matrix by $I_n \in \mathbb{R}^{n\times n}$, the n dimension vector with all elements equal to one by 1_n, $\theta = \text{col}(\theta_i) \in \mathbb{R}^{n_t}$, $\omega = \text{col}(\omega_i) \in \mathbb{R}^n$, $P = \text{col}(P_i) \in \mathbb{R}^{n_t}$ and $\varphi = \text{col}(\varphi_i) \in \mathbb{R}^{n_t}$ where $\varphi_i = \theta_i - \theta_1$ for all $i \in \mathcal{V}$, $\eta = \text{col}(\eta_i) \in \mathbb{R}^n$, and $\xi = \text{col}(\xi_i) \in \mathbb{R}^n$.

The number of the groups is denoted by m, the control price of group r is α_r. Denote $\alpha_R = \text{diag}(\alpha_r) \in \mathbb{R}^{m\times m}$. Define matrix $R = (r_{ir}) \in \mathbb{R}^{n\times m}$ with $r_{ir} = 1$ if node i belongs to group r, otherwise $r_{ir} = 0$. Note that α, α_R, R satisfy

$$R^T \alpha^{-1} R = \alpha_R^{-1}, \tag{66a}$$

$$1_n = R 1_m. \tag{66b}$$

Denote $L \in \mathbb{R}^{m\times m}$ as the Laplacian matrix of the communication network as defined in (10).

For symmetric matrices A and B, we say $A > 0$ (or $A \geq 0$ if A is positive-definite (or semi-positive-definite), and say $A > B$ (or $A \geq B$) if $(A - B)$ is positive-definite (or semi-positive-definite).

The following inequality is used frequently in the following stability analysis of the control laws. For any $x \in \mathbb{R}^m, y \in \mathbb{R}^m$, the following inequality holds

$$x^T y \leq \frac{1}{2} x^T \varepsilon x + \frac{1}{2} y^T \varepsilon^{-1} y,$$

where $\varepsilon \in \mathbb{R}^{m\times m}$ is an invertible positive-definite diagonal matrix. The inequality follows from

$$\begin{bmatrix} x \\ y \end{bmatrix}^T \begin{bmatrix} \varepsilon & -I_m \\ -I_m & \varepsilon^{-1} \end{bmatrix} \begin{bmatrix} x \\ y \end{bmatrix} \geq 0.$$

Appendix B
Preliminaries on DAEs

Consider the following DAE systems

$$\dot{x} = f(x, y), \tag{67a}$$

$$0 = g(x, y), \tag{67b}$$

where $x \in \mathbb{R}^n, y \in \mathbb{R}^m$ and $f : \mathbb{R}^n \times \mathbb{R}^m \to \mathbb{R}^n$ and $g : \mathbb{R}^n \times \mathbb{R}^m \to \mathbb{R}^m$ are twice continuously differentiable functions. $(x(x_0, y_0, t), y(x_0, y_0, t))$ is the solution with the admissible initial conditions (x_0, y_0) satisfying the algebraic constraints

$$0 = g(x_0, y_0), \tag{68}$$

and the maximal domain of a solution of (67) is denoted by $\mathcal{I} \subset \mathbb{R}_{\geq 0}$ where $\mathbb{R}_{\geq 0} = \{x \in \mathbb{R} | x \geq 0\}$.

Before presenting the Lyapunov/LaSalle stability criterion of the DAE system, we make the following two assumptions.

Assumption B.1: The DAE system possesses an equilibrium state (x^*, y^*) such that $f(x^*, y^*) = 0,\ g(x^*, y^*) = 0$.

This article has been accepted for publication in a future issue of this journal, but has not been fully edited. Content may change prior to final publication. Citation information: DOI 10.1109/TAC.2019.2934014, IEEE Transactions on Automatic Control

Assumption B.2: Let $\Omega \subseteq \mathbb{R}^n \times \mathbb{R}^m$ be an open connected set containing (x^*, y^*), assume (67b) is *regular* such that the Jacobian of g with respect to y is a full rank matrix for any $(x, y) \in \Omega$, i.e.,

$$\text{rank}(\nabla_y g(x, y)) = m, \ \forall (x, y) \in \Omega.$$

Assumption (B.2) ensures the existence and uniqueness of the solutions of (67) in Ω over the interval $\mathcal{I}$ with the initial condition (x_0, y_0) satisfying (68).

The following theorem provides a sufficient stability condition for the stability of the equilibrium of DAE in (67).

Theorem B.3: (Lyapunov/LaSalle stability criterion [25], [11]): Consider the DAE system in (67) with assumptions (B.1) and (B.2), and an equilibrium $(x^*, y^*) \in \Omega_H \subset \Omega$. If there exists a continuously differentiable function $H : \Omega_H \to R$, such that (x^*, y^*) is a strict minimum of H i.e., $\nabla H|_{(x^*,y^*)} = 0$ and $\nabla^2 H|_{(x^*,y^*)} > 0$, and $\dot{H}(x, y) \leq 0, \ \forall (x, y) \in \Omega_H$, then the following statements hold:

(1). (x^*, y^*) is a stable equilibrium with a local Lyapunov function $V(x, y) = H(x, y) - H(x^*, y^*) \geq 0$ for (x, y) near (x^*, y^*),

(2). Let $\Omega_c = \{(x, y) \in \Omega_H | H(x, y) \leq c\}$ be a compact sub-level set for a $c > H(x^*, y^*)$. If no solution can stay in $\{(x, y) \in \Omega_c | \dot{H}(x, y) = 0\}$ other than (x^*, y^*), then (x^*, y^*) is asymptotically stable.

We refer to [25] and [11] for the proof of Theorem B.3.

Appendix C
Preliminaries of Symmetrizable matrix

Definition C.1: A matrix $B \in \mathbb{R}^{m\times m}$ is *symmetrizable* if there exists a positive-definite invertible diagonal matrix $A \in \mathbb{R}^{m\times m}$ and a symmetric matrix $L \in \mathbb{R}^{m\times m}$ such that $B = LA$.

Theorem C.2: Consider the Laplacian matrix $L \in \mathbb{R}^{m\times m}$ as defined in (10) and the positive-definite diagonal matrix $\alpha_R \in \mathbb{R}^{m\times m}$ as defined in Appendix (A). The matrix $L\alpha_R$ is a symmetrizable matrix and there exists an invertible matrix Q such that

$$Q^{-1} L \alpha_R Q = \Lambda, \tag{69}$$

where $\Lambda = \text{diag}(\lambda_i) \in \mathbb{R}^{m\times m}$, λ_i is the eigenvalue of $L\alpha$ and $\lambda_1 = 0$. Denote $Q^{-1} = [Q_{v1}, Q_{v2}, \cdots, Q_{vm}]^T$ and $Q = [Q_1, Q_2, \cdots, Q_m]$, we have

$$Q_{v1} = 1_m, \tag{70a}$$
$$\alpha_R Q_1 = 1_m, \tag{70b}$$
$$Q^T \alpha_R Q = I_m, \tag{70c}$$
$$Q^{-1} \alpha_R^{-1} (Q^{-1})^T = I_m, \tag{70d}$$
$$Q^{-1} = Q^T \alpha_R. \tag{70e}$$

Furthermore, the new matrix $W = [Q_{v2}, \cdots, Q_{vm}] \in \mathbb{R}^{n\times(m-1)}$ and $S = [Q_2, \cdots, Q_m] \in \mathbb{R}^{m\times(m-1)}$ satisfy that

$$W^T S = I_{(m-1)}, \tag{71a}$$
$$W^T \alpha_R^{-1} W = I_{(m-1)}, \tag{71b}$$
$$S^T \alpha_R S = I_{(m-1)}, \tag{71c}$$
$$Q_{vi} = \alpha_R Q_i, \tag{71d}$$
$$W = \alpha_R S. \tag{71e}$$

Proof: Let $T = \sqrt{\alpha_R}$ which is a diagonal matrix, then

$$T L \alpha_R T^{-1} = \sqrt{\alpha_R} L \sqrt{\alpha_R}.$$

Hence, there exists an invertible matrix $\Gamma^{-1} = \Gamma^T$ such that

$$\Gamma^{-1} T L \alpha_R T^{-1} \Gamma = \Gamma^{-1} \sqrt{\alpha_R} L \sqrt{\alpha_R} \Gamma = \Lambda.$$

Let $Q = T^{-1}\Gamma$, we derive $Q^{-1} L \alpha_R Q = \Lambda$. Since L is a Laplacian matrix as defined in (10), we have $1_m^T L \alpha_R = 0$, then there is a zero eigenvalue, i.e., $\lambda_1 = 0$. Denote $\Gamma = [\Gamma_1, \Gamma_2, \cdots, \Gamma_m]$, then $\Gamma^{-1} = \Gamma^T = [\Gamma_1, \Gamma_2, \cdots, \Gamma_m]^T$.

Since Γ_1 is the eigenvector corresponding to $\lambda_1 = 0$ of $\sqrt{\alpha_R} L \sqrt{\alpha_R}$ such that $L\sqrt{\alpha_R}\Gamma_1 = 0$, from which we derive $\sqrt{\alpha_R}\Gamma_1 = 1_m$. Hence by $Q = T^{-1}\Gamma$, we obtain $Q_1 = (\sqrt{\alpha_R})^{-1}\Gamma_1 = \alpha_R^{-1} 1_m$. Similarly we derive $Q_{v1} = \Gamma_1^T T = \Gamma^T \sqrt{\alpha_R} = \sqrt{\alpha_R}\Gamma_1 = 1_m$.

By $Q = T^{-1}\Gamma$, we derive $\Gamma^T \alpha_R Q = \Gamma^T T^{-1} \alpha_R T^{-1} \Gamma = I_m$. $Q^{-1}\alpha_R^{-1}(Q^{-1})^T = R^T R = I_m$ can be obtained similarly.

(71a) is yielded directly from $Q^{-1}Q = I_m$. (70c) and (70d) yields (71b) and (71c). □

References

[1] M. Andreasson, D. V. Dimarogonas, H. Sandberg, and K. H. Johansson. Distributed control of networked dynamical systems: Static feedback, integral action and consensus. *IEEE Trans. Autom. Control*, 59(7):1750–1764, 2014.

[2] A. Araposthatis, S. Sastry, and P. Varaiya. Analysis of power-flow equation. *Int. J. Elec. Power*, 3(3):115–126, 1981.

[3] T. Athay, R. Podmore, and S. Virmani. A practical method for the direct analysis of transient stability. *IEEE Trans. Power App. Syst.*, PAS-98(2):573–584, 1979.

[4] A. W. Berger and F. C. Schweppe. Real time pricing to assist in load frequency control. *IEEE Trans. Power Syst.*, 4(3):920–926, 1989.

[5] H. Bevrani. *Robust Power System Frequency Control*. Springer, 2nd edition, 2014.

[6] F. Dörfler and F. Bullo. Synchronization in complex networks of phase oscillators: A survey. *Automatica*, 50(6):1539 – 1564, 2014.

[7] F. Dörfler and S. Grammatico. Gather-and-broadcast frequency control in power systems. *Automatica*, 79:296 – 305, 2017.

[8] F. Dörfler, J. W. Simpson-Porco, and F. Bullo. Breaking the hierarchy: distributed control and economic optimality in microgrids. *IEEE Trans. Control Netw. Syst.*, 3(3):241–253, 2016.

[9] O. I. Elgerd and C. E. Fosha. Optimum megawatt-frequency control of multiarea electric energy systems. *IEEE Trans. Power App. Syst.*, PAS-89(4):556–563, 1970.

[10] Ertu grul Cam and Ilhan Kocaarslan. Load frequency control in two area power systems using fuzzy logic controller. *Energy Convers. Manag.*, 46(2):233 – 243, 2005.

[11] D. J. Hill and I. M. Y. Mareels. Stability theory for differential algebraic systems with applications to power systems. *IEEE Trans. Circuits Syst.*, 37(11):1416–1423, 1990.

[12] Ibraheem, P. Kumar, and D. P. Kothari. Recent philosophies of automatic generation control strategies in power systems. *IEEE Trans. Power Syst.*, 20(1):346–357, 2005.

[13] M.D. Ilić and J. Zaborszky. *Dynamics and control of large electric power systems*. John Wiley & Sons, 2000.

[14] H. K. Khalil. *Nonlinear Systems*. Prentice Hall, 2002.

[15] P. Kundur. *Power system stability and control*. McGraw-Hill, 1994.

[16] N. Li, C. Zhao, and L. Chen. Connecting automatic generation control and economic dispatch from an optimization view. *IEEE Trans. Control Netw. Syst.*, 3(3):254–263, 2016.

[17] Y. Liu, Z. Qu, H. Xin, and D. Gan. Distributed real-time optimal power flow control in smart grid. *IEEE Trans. Power Syst.*, 32(5):3403–3414, 2017.

[18] Y. Mi, Y. Fu, C. Wang, and P. Wang. Decentralized sliding mode load frequency control for multi-area power systems. *IEEE Trans. Power Syst.*, 28(4):4301–4309, 2013.

[19] F. Milano. *Power system analysis toolbox*. University of Castilla, Castilla-La Mancha, Spain, 2008.

[20] D. K. Molzahn, F. Dörfler, H. Sandberg, S. H. Low, S. Chakrabarti, R. Baldick, and J. Lavaei. A survey of distributed optimization and control algorithms for electric power systems. *IEEE Trans. Smart Grid*, 8(6):2941–2962, 2017.

[21] A. E. Motter, S. A. Myers, M. Anghel, and T. Nishikawa. Spontaneous synchrony in power-grid networks. *Nat. Phys.*, 9(3):191–197, 2013.

[22] North Amertican Electric Reliablity Corporation. Balancing and frequency control: A technical document prepared by the NERC resource subcommittee. 2011.

[23] C. De Persis and N. Monshizadeh. Bregman storage functions for microgrid control. *IEEE Trans. Autom. Control*, 63(1):53–68, 2018.

[24] D. Rerkpreedapong, A. Hasanovic, and A. Feliachi. Robust load frequency control using genetic algorithms and linear matrix inequalities. *IEEE Trans. Power Syst.*, 18(2):855–861, 2003.

[25] J. Schiffer and F. Dörfler. On stability of a distributed averaging pi frequency and active power controlled differential-algebraic power system model. In *Proc. 2016 Eur. Control Conf.*, pages 1487–1492, 2016.

[26] J. Schiffer, F. Dörfler, and E. Fridman. Robustness of distributed averaging control in power systems: Time delays & dynamic communication topology. *Automatica*, 80:261–271, 2017.

[27] Q. Shafiee, J. M. Guerrero, and J. C. Vasquez. Distributed secondary control for islanded microgrids-a novel approach. *IEEE Trans. Power Electron.*, 29(2):1018–1031, 2014.

[28] J. W. Simpson-Porco, Q. Shafiee, F. Dörfler, J. C. Vasquez, J. M. Guerrero, and F. Bullo. Secondary frequency and voltage control of islanded microgrids via distributed averaging. *IEEE Trans. Ind. Electron.*, 62(11):7025–7038, 2015.

[29] S. J. Skar. Stability of multi-machine power systems with nontrivial transfer conductances. *SIAM J. Appl. Math.*, 39(3):475–491, 1980.

[30] S. Trip, M. Bürger, and C. De Persis. An internal model approach to (optimal) frequency regulation in power grids with time-varying voltages. *Automatica*, 64:240 – 253, 2016.

[31] S. Trip and C. De Persis. Optimal frequency regulation in nonlinear structure preserving power networks including turbine dynamics: An incremental passivity approach. In *Prof. 2016 Amer. Control Conf.*, pages 4132–4137, 2016.

[32] S. Trip and C. De Persis. Communication requirements in a master-slave control structure for optimal load frequency control. *IFAC-PapersOnLine*, 50(1):10102 – 10107, 2017.

[33] P. van Mieghem. *Graph Spectra for Complex Networks*. Cambridge University Press, 2011.

[34] K. Vrdoljak, N. Perić, and I. Petrović. Sliding mode based load-frequency control in power systems. *Electr. Pow. Syst. Res.*, 80(5):514 – 527, 2010.

[35] Z. Wang, F. Liu, S. H. Low, C. Zhao, and S. Mei. Distributed frequency control with operational constraints, part II: Network power balance. *IEEE Trans. Smart Grid*, 10(1):53–64, 2019.

[36] A. J. Wood and B. F. Wollenberg. *Power generation, operation, and control*. John Wiley & Sons, 2nd edition, 1996.

[37] X. Wu and C. Shen. Distributed optimal control for stability enhancement of microgrids with multiple distributed generators. *IEEE Trans. Power Syst.*, 32(5):4045–4059, 2017.

[38] X. Wu, C. Shen, and R. Iravani. A distributed, cooperative frequency and voltage control for microgrids. *IEEE Trans. Smart Grid*, 9(4):2764–2776, 2018.

[39] K. Xi, J. L. A. Dubbeldam, and H. X. Lin. Synchronization of cyclic power grids: equilibria and stability of the synchronous state. *Chaos*, 27(1):013109, 2017.

[40] K. Xi, J. L.A. Dubbeldam, H. X. Lin, and J. H. van Schuppen. Power-imbalance allocation control for secondary frequency control of power systems. *IFAC-PapersOnLine*, 50(1):4382 – 4387, 2017.

[41] K. Xi, H. X. Lin, and J. H. van Schuppen. Power-imbalance allocation control of frequency control of power systems-a frequency bound for time-varying loads. In *Proc. 36th Chinese Control Conf.*, pages 10528–10533, 2017.

[42] K. Xi, H. X. Lin, and J. H. van Schuppen. Power imbalance allocation control of power systems-secondary frequency control. *Automatica*, 92:72–85, 2018.

[43] C. Zhao, E. Mallada, and F. Dörfler. Distributed frequency control for stability and economic dispatch in power networks. In *Proc. 2015 Amer. Control Conf.*, pages 2359–2364, July 2015.

[44] C. Zhao, E. Mallada, S. Low, and J. Bialek. A unified framework for frequency control and congestion management. In *Proc. 2016 Power Syst. Comp. Conf.*, pages 1–7, 2016.

Kaihua Xi (M'19) received the PhD in Delft Institute of Applied mathematics of Delft University of Technology, Delft, The Netherlands, in June 2018, and received the M.Sc in computational mathematics in Shandong University, Jinan, China, in June 2010. He was a research assistant in the School of Mathematics, Shandong University, from 2010 to 2013.

He is an assistant professor in the school of mathematics, Shandong University, Jinan, China. His research includes control, optimization and stability analysis of power systems, numerical analysis and optimal control of Partial Differential Equations, and high performance computing of large-scale systems.

Hai Xiang Lin is an associate professor at TU Delft working in the mathematical physics area at the Delft Institute of Applied Mathematics (DIAM). He is also appointed as a professor in Data Analytics for Environmental Modelling at Institute of Environmental Sciences, Leiden University on behalf of the R. Timman foundation.

His research interests include parallel numerical algorithms (sparse matrix computation), parallel data assimilation algorithms, simulation and control of power systems, modelling and simulation of environmental pollution, machine learning and big data. He has published more than 100 peer reviewed journal and international conference papers, he is an associate editor of the journal Algorithms and Computational Technology (JACT). Furthermore, he is teaching Master and PhD courses in High performance computing, Parallel computing, Scientific programming and Computational aspects of stochastic differential equations.

Chen Shen (M'98-SM'07) received the B.E. degree in electrical power engineering and the Ph.D degree in electrical power engineering from Tsinghua University in 1993 and 1998, respectively. Since 2009, he has been a professor in the Electrical Engineering Department with Tsinghua University, where he is currently the Director of Power System Research Institute with the Department of Electrical Engineering. His research focuses on power systems analysis and control, including fast modeling and simulation of smart grids, stability analysis of power system with wind generation, emergency control and risk assessment of power systems, planning, simulation operation, and control of micro-grids.

Jan H. van Schuppen (M'71-LM'13) received the Engineering Diploma from the Department of Applied Physics, Delft University of Technology, Delft, The Netherlands, in 1970 and the Ph.D. from the Department of Electrical Engineering and Computer Science, University of California, Berkeley, CA, USA, in 1973.

He is affiliated as a Professor Emeritus with the Department of Mathematics, Delft University of Technology, Delft, The Netherlands, and as a Director and Researcher with his consulting company, Van Schuppen Control Research, in Amsterdam, The Netherlands, since his retirement in October 2012. His research includes: control of decentralized and distributed systems,control of hybrid systems, control of discrete-event systems, realization, system identification,control of motorway networks, and modeling and identification of biochemical reaction networks. He was coordinator of the C4C Project *Control for coordination of distributed systems* which was financially supported in part by the European Commission.

Dr. van Schuppen is a Fellow of the research institute Centrum Wiskunde and Informatica (CWI), Amsterdam. He is a member of the IEEE Societies of Control Systems, Computer, and Information Theory, and of the Society for Industrial and Applied Mathematics (SIAM). He is a co-editor of the journal Mathematics of Control, Signal, and Systems, was an associate-editor-at-large of the IEEE TRANSACTIONS ON AUTOMATIC CONTROL, and was a Department Editor of *Discrete-event Dynamics Systems*